# ON THE STABILITY OF FULLY ADAPTIVE MULTISCALE SCHEMES FOR CONSERVATION LAWS USING APPROXIMATE FLUX AND SOURCE RECONSTRUCTION STRATEGIES*

NUNE HOVHANNISYAN† AND SIEGFRIED MÜLLER‡

**Abstract.** In order to accelerate finite volume schemes applied to (inhomogeneous) hyperbolic conservation laws multiresolution based adaptive concepts can be used. The basic idea is to analyze the local regularity by means of a multiresolution analysis of cell averages. By difference information between successive refinement levels local grid adaptation is triggered employing threshold techniques. This leads to a significant gain in computational complexity. The crux is to compute numerical fluxes and sources on local resolution levels such that the overall accuracy of the reference solution on the finest discretization is maintained. In the present work a modified approach based on polynomial reconstruction techniques is introduced and investigated analytically. The efficiency and accuracy of the adaptive concept is significantly improved, in particular for inhomogeneous equations. This is confirmed by numerical parameter studies.

**Key words.** conservation laws, finite volume schemes, grid adaptation, biorthogonal wavelets

**AMS subject classifications.** 35L65, 65M12, 65M50, 65T60, 74S10

**1. Introduction.** Nowadays finite volume methods are routinely used for the discretization of conservation laws as they arise, for instance, in computational fluid dynamics. Here, due to the inhomogeneity of the solutions, adaptive grid methods can significantly improve the efficiency by concentrating cells only where they are most required, while reducing storage requirements as well as the computational time.

For this purpose, numerical schemes have been discussed or are under current investigation that aim at adapting the *spatial* grid to the local behavior of the flow field. In the early 90's Harten [13] proposed to use *multiresolution techniques*. The cell averages on a given highest level of resolution (*reference mesh*) are represented as cell averages on some coarse level where the fine scale information is encoded in arrays of *detail coefficients* of ascending resolution that reveals insight into the local behavior of the solution. This multiresolution framework has been extended to multidimensional problems [3, 1, 10, 8, 20] on Cartesian, curvilinear and unstructured meshes, respectively.

In Harten's original approach the multiresolution analysis is used to control a hybrid flux computation by which computational time for the flux computation can be saved whereas the overall computational complexity is not reduced but still stays proportional to the number of cells on the uniformly fine reference mesh. Opposite to this strategy, threshold techniques are applied to the multiresolution decomposition in [12, 18, 9, 16, 21] where detail coefficients below a threshold value are discarded. By means of the remaining significant details a locally refined mesh is determined whose complexity is significantly reduced in comparison to the underlying reference mesh. A comparison of Harten's original framework and the fully adaptive framework can be found in [6].

*This work has been performed with funding by the Deutsche Forschungsgemeinschaft in the Collaborative Research Center SFB 401 "Flow Modulation and Fluid-Structure Interaction at Airplane Wings" of the RWTH Aachen, University of Technology, Aachen, Germany.

†Institut für Geometrie und Praktische Mathematik, RWTH Aachen, Templergraben 55, D-52056 Aachen, Germany (nune@igpm.rwth-aachen.de).

‡Institut für Geometrie und Praktische Mathematik, RWTH Aachen, Templergraben 55, D-52056 Aachen, Germany (mueller@igpm.rwth-aachen.de).

**Objective**. The central mathematical problem is to verify that the solution computed on the locally adapted mesh provides an accuracy that is of the same order as the one of the reference scheme on the reference mesh. This has been analytically investigated in the context of a *homogeneous* scalar conservation law in one space dimension, see [18, 9]. The proof relies essentially on (i) the strategy how to predict significant details at the new time level from the data at the old time level in order to locally refine the grid before the time evolution and (ii) the interpretation of the adaptive scheme as the original finite volume scheme on the reference grid (*reference scheme*) to which we apply the multiresolution analysis and thresholding. The second property only holds true provided that the numerical fluxes are computed by data at the *highest* spatial level employing a local inverse multiresolution transformation. This local flux computation strategy is referred to as the *exact flux reconstruction strategy*. In higher dimensional applications it will increase the computational complexity. In particular, for *inhomogeneous* conservation laws taking into account some source term the *exact* strategy requires the computation of all sources on the *reference* grid rather than the *adaptive* grid. This would completely deteriorate the efficiency of the adaptive scheme.

The main purpose of the present work is to suggest an *approximate flux and source reconstruction strategy*. The basic idea is to compute to each cell in the adaptive grid a reconstruction polynomial by which we provide the data for the computation of the local fluxes. Moreover, the local sources are determined by a quadrature rule applied to the composite of the source function and the reconstruction polynomial. This strategy does not spoil the computational complexity of the adaptive scheme even in higher dimensions. We will verify analytically that by the suggested strategy the accuracy of the reference scheme can be maintained. In particular, we prove that by the evolution process on the adaptive grid using the approximate reconstruction strategy we introduce an additional error in comparison to the evolution with exact reconstruction that is proportional to the threshold value.

**Reference scheme**. In order to simplify the notation we confine ourselves to the one-dimensional case although the concepts extend to higher dimensional problems as well and have been successfully applied to complex configurations in fluid dynamics, e.g. [4] for the classical fully adaptive finite volume scheme. We therefore consider the scalar *inhomogeneous* conservation law

$$u_t(t,x) + (f(u(t,x)))_x = s(u(t,x)), \quad t > 0,\ x \in \mathbb{R}, \tag{1.1}$$

subject to the initial condition

$$u(0,x) = u_0(x), \quad x \in \mathbb{R}. \tag{1.2}$$

If $u_0 \in L^\infty(\mathbb{R}) \cap L^1(\mathbb{R})$ and the flux $f : \mathbb{R} \to \mathbb{R}$ and the source $s : \mathbb{R} \to \mathbb{R}$ are such that all derivatives up to the second order exist and are bounded, then there exists a unique entropy solution, see [19, 17].

A conservative finite volume discretization of the initial value problem (1.1), (1.2) can be written in the form

$$v_k^{n+1} = v_k^n - \lambda\, B_k^n + \tau S_k^n, \quad \lambda := \frac{\tau}{h} \tag{1.3}$$

for the cell averages $v_k$. Here space and time are uniformly discretized by $h$ and $\tau$, respectively. Conservation means that the flux balance $B_k^n$ has the form

$$B_k^n := F(v_{k-p+1}^n, \dots, v_{k+p}^n) - F(v_{k-p}^n, \dots, v_{k+p-1}^n) = F_{k+1}^n - F_k^n \tag{1.4}$$

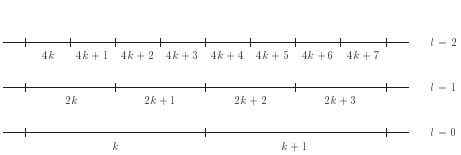


FIG. 2.1. *Dyadic grid hierarchy*

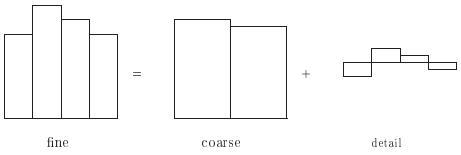


FIG. 2.2. *Two-scale decomposition*

where the function $F(u_1, \ldots, u_{2p})$ is the numerical flux function. The source term is approximated by the numerical source function $S$. For simplicity of representation, we confine ourselves to the first order approximation

$$S_k^n \equiv S(v_k^n) := s(v_k^n). \tag{1.5}$$

Later on we will specify assumptions on $F$ and $S$ that will guarantee the convergence of the scheme.

**Outline**. In the following we first summarize the multiresolution analysis (MRA) in Section 2. Then in Section 3 the MRA is employed to compress the set of evolution equations given by a reference finite volume scheme on the reference grid in order to reduce the computational costs both in terms of CPU and memory. A new strategy is introduced in Section 4 for the computation of the local numerical fluxes and sources on coarser discretization levels that is based on polynomial reconstruction. In Section 5 we verify that by the approximate flux and source reconstruction strategy the accuracy of the reference finite volume scheme can be maintained. Finally, in Section 6, we perform numerical parameter studies for the inviscid Burgers equation comparing different strategies for the local computation of the numerical fluxes and sources.

**2. Multiresolution analysis.** A finite volume discretization is typically working on a sequence of cell averages. In order to analyze the local regularity behavior of the data we decompose this sequence into coarse grid information and detail information describing the update from low to high resolution. This new data format can be compressed by thresholding because the details become small when the solution is locally smooth. By means of the compressed data a locally refined grid is determined. To provide the MRA of the data one might used either the concept of biorthogonal wavelets [5] or Harten's discrete framework [14, 2] based on reconstruction and prediction. These concepts are linked by the convergence of subdivision schemes.

**Grid hierarchy**. Starting point for the construction of a MRA is a sequence of nested grids. Here we confine ourselves to 1D dyadic grid refinements. For an extension to grid hierarchies in higher dimensions we refer to [18]. Let be $\mathcal{G}_l := \{V_{l,k}\}_{k \in I_l}$, $l \in \mathbb{N}_0$, $I_l = \mathbb{Z}$, a sequence of grids with increasing resolution. These meshes are composed of the intervals $V_{l,k} = [x_{l,k}, x_{l,k+1}]$ determined by the grid points $x_{l,k} = 2^{-l} k$, $k \in \mathbb{Z}$ with interval length $h_l = 2^{-l}$. Hence, the resulting grid hierarchy is *nested* because of the subdivision condition

$$V_{l,k} = V_{l+1,2k} \cup V_{l+1,2k+1}, \qquad \forall\, l \in \mathbb{N}_0,\ k \in \mathbb{Z}. \tag{2.1}$$

The dyadic grid refinement is illustrated in Figure 2.1.

**Cell averages and details**. Relative to the partitions $\mathcal{G}_l$ we introduce the averages of a scalar, integrable function $u \in L^1(\Omega)$

$$\hat{u}_{l,k} := \frac{1}{|V_{l,k}|} \int_{V_{l,k}} u \, dx. \tag{2.2}$$

Obviously the nestedness of the grids as well as the linearity of integration imply the two–scale relation

$$\hat{u}_{l,k} = \frac{1}{2}(\hat{u}_{l+1,2k} + \hat{u}_{l+1,2k+1}) =: \sum_{r \in \mathcal{M}^0_{l,k}} m^{l,0}_{r,k}\, \hat{u}_{l+1,r} \tag{2.3}$$

where for later use we introduce the mask coefficients $m^{l,0}_{r,k} := 0.5$ and their support index $\mathcal{M}^0_{l,k} = \{2k, 2k+1\}$. An error between level $l$ and $l+1$ can be introduced by

$$e_{l,2k} = \hat{u}_{l+1,2k} - \hat{u}_{l,k}, \quad e_{l,2k+1} = \hat{u}_{l+1,2k+1} - \hat{u}_{l,k}.$$

These are two options for one missing information to recompute the data on higher scale. To remove the redundancy a linear combination of the errors

$$d_{l,k} := \frac{1}{2}\,(e_{l,2k} - e_{l,2k+1}) = \frac{1}{2}(\hat{u}_{l+1,2k} - \hat{u}_{l+1,2k+1}) \tag{2.4}$$

can be introduced. Then the system of equations (2.3) and (2.4) is regular and we obtain the inverse two-scale relation

$$\hat{u}_{l+1,2k+i} = \hat{u}_{l,k} + d_{l,k}, \quad \hat{u}_{l+1,2k+i} = \hat{u}_{l,k} - d_{l,k}. \tag{2.5}$$

**Cancellation Property**. Obviously, the detail vanishes if the underlying function $u$ is a constant, see also Figure 2.2. This motivates to neglect all sufficiently small details in order to compress the original data. For general $u$, it can be shown that the details become small with increasing refinement level when the underlying function is smooth. Higher compression rates can be realized if the details vanish for higher order polynomials up to some degree $M-1$ as well because the decay is proportional to $2^{-l\,M}$. This corresponds to higher order vanishing moments in the wavelet framework, e.g. [7].

**Higher vanishing moments**. In order to realize higher vanishing moments we introduce additional parameters in (2.5) by a coarse grid modification, i.e.,

$$d_{l,k} = \frac{1}{2}(\hat{u}_{l+1,2k} - \hat{u}_{l+1,2k+1}) + \sum_{r=0}^{2s} l_r \hat{u}_{l,k-s+r} = \sum_{r \in \mathcal{M}^1_{l,k}} m^{l,1}_{r,k}\, \hat{u}_{l+1,r}. \tag{2.6}$$

By means of (2.3) the coarse grid averages $\hat{u}_{l,k-s+r}$ can be rewritten in terms of the fine grid averages $\hat{u}_{l+1,r}$ characterizing the mask coefficients $m^{l,1}_{r,k}$ and the support index $\mathcal{M}^1_{l,k}$. These parameters are then chosen such that the details vanish for polynomials up to degree $2s$, i.e., $M = 2s+1$. In the wavelet framework this procedure is referred to the *change of stable completion* [5] or *second generation wavelets* [22]. For some $s$ the resulting parameters are listed in Table 2.1. In case of $s = 0$ these correspond to the Haar wavelet. For our computations we only use $s = 1, 2$; for $s = 0$ the adaptive scheme does not work at all. The inverse two-scale relation then reads

$$\begin{aligned} \hat{u}_{l+1,2k+i} &= \hat{u}_{l,k} + (-1)^i d_{l,k} + (-1)^{i+1} \sum_{r=-s}^{s} l_{r+s} \hat{u}_{l,k+r} \\ &=: \sum_{r \in \mathcal{G}^0_{l,2k+i}} g^{l,0}_{r,2k+i}\, \hat{u}_{l,r} + \sum_{r \in \mathcal{G}^1_{l,2k+i}} g^{l,1}_{r,2k+i}\, d_{l,r}, \quad i = 0, 1 \end{aligned} \tag{2.7}$$

TABLE 2.1
*Lifting coefficients*

| $s$ | $l_0$ | $l_1$ | $l_2$ | $l_3$ | $l_4$ |
|---|---|---|---|---|---|
| 0 | 0 | | | | |
| 1 | -1/8 | 0 | 1/8 | | |
| 2 | 3/128 | -11/64 | 0 | 11/64 | -3/128 |

with mask coefficients $g^{l,e}_{r,2k+i}$ and corresponding support $\mathcal{G}^e_{l,2k+i}$, $e = 0, 1$.

**Multiscale Transformation**. Recursively applying the two-scale relations (2.3) and (2.6) array of cell averages $\mathbf{u}_L := (\hat{u}_{L,k})_{k\in I_L}$ corresponding to a finest uniform discretization level is transformed successively into a sequence of coarse grid data $\mathbf{u}_0 := (\hat{u}_{0,k})_{k\in I_0}$ and details $\mathbf{d}_l := (d_{l,k})_{k\in I_l}$, $l = 0, \ldots, L-1$. We refer to this transformation as *multiscale transformation* determined by the multiscale operator $\mathcal{M}_L : \hat{\mathbf{u}}_L \longrightarrow (\hat{\mathbf{u}}_0, \mathbf{d}_0, \ldots, \mathbf{d}_{L-1})$ with

$$\hat{\mathbf{u}}_l = \mathbf{M}^T_{l,0}\hat{\mathbf{u}}_{l+1}, \quad \mathbf{d}_l = \mathbf{M}^T_{l,1}\hat{\mathbf{u}}_{l+1}.$$

It is reversed by recursively applying the two-scale relation (2.7). The resulting *inverse multiscale transformation* is described by inverse multiscale operator $\mathcal{M}_L^{-1} : (\hat{\mathbf{u}}_0, \mathbf{d}_0, \ldots, \mathbf{d}_{L-1}) \longrightarrow \hat{\mathbf{u}}_L$ with

$$\hat{\mathbf{u}}_{l+1} = \mathbf{G}^T_{l,0}\hat{\mathbf{u}}_l + \mathbf{G}^T_{l,1}\mathbf{d}_l.$$

**Subdivision scheme**. By means of the inverse multiscale transformation the array of cell averages $\mathbf{u}_L$ can be transformed to

$$\hat{\mathbf{u}}_L = \mathbf{G}^L_{l,0}\hat{\mathbf{u}}_l + \sum_{j=l}^{L-1} \mathbf{G}^L_{j,1}\mathbf{d}_j = \sum_{k\in I_l} \mathbf{\Psi}^L_{l,k,0}\hat{u}_{l,k} + \sum_{j=l}^{L-1}\sum_{k\in I_l} \mathbf{\Psi}^L_{j,k,1} d_{j,k}, \tag{2.8}$$

for $l = 0, \ldots, L-1$ where the *subdivision procedure* is determined by the matrices $\mathbf{G}^L_{l,e} := \mathbf{G}^T_{L-1,0} \cdot \ldots \cdot \mathbf{G}^T_{l+1,0}\mathbf{G}^T_{l,e}$, $e \in \{0, 1\}$. The vectors $\mathbf{\Psi}^L_{l,k,e} := \mathbf{G}^L_{l,1,e}\mathbf{c}_{l,k}$ with the Dirac vector $\mathbf{c}_{l,k} = (\delta_{k,r})_{r\in I_l}$ denote the $k$-th column of the subdivision procedure. These are sparse because of the inverse two-scale relation (2.7). Their supports

$$\bar{\Sigma}^{(l)}_{L,k,e} := \operatorname{supp}(\mathbf{\Psi}^L_{l,k,e})$$

are uniformly bounded by

$$\begin{aligned}
\bar{\Sigma}^{(L-1)}_{L,k,0} &= \left\{ \left\lfloor \frac{k}{2} \right\rfloor - s, \ldots, \left\lfloor \frac{k}{2} \right\rfloor + s \right\}, \quad \bar{\Sigma}^{(l)}_{L,k,0} \subset \left\{ \left\lfloor \frac{k}{2^{L-l}} \right\rfloor - 2s, \ldots, \left\lfloor \frac{k}{2^{L-l}} \right\rfloor + 2s \right\} \\
\bar{\Sigma}^{(L-1)}_{L,k,1} &= \left\{ \left\lfloor \frac{k}{2} \right\rfloor \right\}, \quad \bar{\Sigma}^{(l)}_{L,k,1} \subset \left\{ \left\lfloor \frac{k}{2^{L-l}} \right\rfloor - s, \ldots, \left\lfloor \frac{k}{2^{L-l}} \right\rfloor + s \right\}
\end{aligned} \tag{2.9}$$

for $0 \le l < L-1$. If the subdivision scheme converges then there is a link between the discrete framework and biorthogonal wavelets summarized in the following

THEOREM 2.1. *(Biorthogonal wavelet decompositions) Assume that the piecewise constant functions $\psi^L_{j,k,e}$, $e \in \{0, 1\}$ defined by*

$$\psi^L_{j,k,e}(x) := (\mathbf{\Psi}^L_{j,k,e})_r, \ x \in V_{L,r}, \ r \in I_L \tag{2.10}$$

*converge uniformly in $L$ towards a function $\psi_{j,k,e} \in L^\infty(\Omega)$ in the sup–norm. Then the limit functions (primal scaling functions ($e = 0$) resp. wavelets ($e = 1$)) satisfy the following properties:*

*1.) Any function $u \in L^\infty(\Omega)$ can be uniquely expanded in a series of the primal wavelet basis, i.e.,*

$$u = \sum_{k \in I_0} \langle u, \tilde{\psi}_{0,k,0} \rangle_{L^2} \, \psi_{0,k,0} + \sum_{j \in \mathbb{N}} \sum_{k \in I_j} \langle u, \tilde{\psi}_{j,k,1} \rangle_{L^2} \, \psi_{j,k,1};$$

*2.) the primal wavelets satisfy the duality relation*

$$\langle \psi_{j,k,e}, \tilde{\psi}_{j',k',e'} \rangle_{L^2} = \delta_{(j,k,e),(j',k',e')};$$

*3.) the components of the discrete basis vectors coincide with the averages of the function $\psi_{j,k,e}$, i.e.,*

$$\mathbf{\Psi}^L_{j,k,e} = (\langle \psi_{j,k,e}, \tilde{\phi}_{L,r} \rangle)_{r \in I_L};$$

*4.) the functions $\psi_{j,k,e}$ are uniformly bounded in the sup–norm, i.e., there exists a constant $C > 0$ independent of $j$, $k$ and $e$ such that*

$$\|\psi_{j,k,e}\|_{L^\infty} < C;$$

*5.) if the grid is quasi–uniform and the mask matrices $\mathbf{G}_{j,e}$ are uniformly banded, then the functions $\psi_{j,k,e}$ are compactly supported and, in particular,*

$$|\operatorname{supp} \psi_{j,k,e}| \leq C \, 2^{-jd}.$$

A proof can be found in [7].

**Thresholding and approximation**. Due to the cancellation property the details might become negligible small whenever the underlying function is locally smooth. This gives rise to hard thresholding characterized by the index set

$$\mathcal{D}_{\boldsymbol{\varepsilon}} := \{(l,k,1) \, : \, |d_{l,k}| > \varepsilon_l\} \cup \{(0,k,0) \, : \, |\hat{u}_{0,k}| > \varepsilon_0\}.$$

Here $\boldsymbol{\varepsilon}$ denotes the vector of level-dependent threshold values. Then the threshold operator $\mathcal{T}_{\mathcal{D}_{\boldsymbol{\varepsilon}}} : (\hat{\mathbf{u}}_0, \mathbf{d}_0, \ldots, \mathbf{d}_{L-1}) \longrightarrow (\tilde{\mathbf{u}}_0, \tilde{\mathbf{d}}_0, \ldots, \tilde{\mathbf{d}}_{L-1})$ is defined elementwise by

$$\tilde{d}_{l,k} := \begin{cases} d_{l,k} & , \quad (l,k,1) \in \mathcal{D}_{\boldsymbol{\varepsilon}}, \\ 0 & , \quad \text{else} \end{cases} \qquad \tilde{u}_{0,k} := \begin{cases} \hat{u}_{0,k} & , \quad (0,k,0) \in \mathcal{D}_{\boldsymbol{\varepsilon}}, \\ 0 & , \quad \text{else} \end{cases}.$$

Later on we will not only perform thresholding by the set $\mathcal{D}_{\boldsymbol{\varepsilon}}$ but by an arbitrary index set $\mathcal{D}$. Then the approximation error due to thresholding is determined by

$$\hat{\mathbf{u}}_L - \mathcal{A}_{\mathcal{D}} \, \hat{\mathbf{u}}_L = \sum_{(j,k,e) \notin \mathcal{D}} \mathbf{\Psi}^L_{j,k,e} \, d_{j,k,e} \tag{2.11}$$

where $\mathcal{A}_{\mathcal{D}} := \mathcal{M}_L^{-1} \, \mathcal{T}_{\mathcal{D}} \, \mathcal{M}_L$ and, in particular for $\mathcal{D} = \mathcal{D}_{\boldsymbol{\varepsilon}}$, $\mathcal{A}_{\boldsymbol{\varepsilon}} := \mathcal{M}_L^{-1} \, \mathcal{T}_{\mathcal{D}_{\boldsymbol{\varepsilon}}} \, \mathcal{M}_L$. In order to control the perturbation error we need convergence of the subdivision scheme at least in the $l^1$–metric, see Theorem 2.1.

**3. From the reference scheme to an adaptive scheme.** We will briefly summarize how to accelerate a finite volume scheme by means of a MRA and data compression via thresholding. For this purpose we first apply the multiscale transformation (2.3) and (2.7) to the evolution equations (1.3) on the uniform reference mesh, i.e., $k \in I_L$. This gives the evolution equations for the cell averages

$$v^{n+1}_{l,k} = v^n_{l,k} - \lambda_l B^n_{l,k} + \tau \, S^n_{l,k} \tag{3.1}$$

and the multiscale coefficients, respectively,

$$v_{0,k}^{n+1} = v_{0,k}^n - \sum_{r\in\mathcal{M}_{0,k}^0} m_{r,k}^{0,0}\,\lambda_1\,B_{1,r}^n + \tau \sum_{r\in\mathcal{M}_{0,k}^0} m_{r,k}^{0,0}\overline{S}_{1,r}^n, \tag{3.2}$$

$$d_{l,k}^{n+1} = d_{l,k}^n - \sum_{r\in\mathcal{M}_{l,k}^1} m_{r,k}^{l,1}\,\lambda_{l+1}\,B_{l+1,r}^n + \tau \sum_{r\in\mathcal{M}_{l,k}^1} m_{r,k}^{l,1}\overline{S}_{l+1,r}^n. \tag{3.3}$$

Here the numerical fluxes $F_{l,k}^n$, respectively the numerical flux balances $B_{l,k}^n := F_{l,k+1}^n - F_{l,k}^n$ and numerical sources $\overline{S}_{l,k}^n$ are recursively defined from fine to coarse scale via

$$F_{l,k}^n = F_{l+1,2k}^n = \ldots = F_{L,2^{L-l}k}^n = F(v_{L,2^{L-l}k-p}^n,\ldots,v_{L,2^{L-l}k+p-1}^n), \tag{3.4}$$

$$\overline{S}_{l,k}^n = 2^{-1}\sum_{r\in\mathcal{M}_{l,k}^0} \overline{S}_{l+1,r}^n = 2^{l-L}\sum_{i=0}^{2^{L-l}-1} \overline{S}_{L,2^{L-l}k+i}^n = 2^{l-L}\sum_{i=0}^{2^{L-l}-1} S(v_{L,2^{L-l}k+i}^n). \tag{3.5}$$

Note that due to the nestedness of the grid hierarchy and the conservation property of the numerical fluxes, the coarse-scale flux balances are only computed by the fine-scale fluxes corresponding to the edges of the coarse cell, see (3.4). These, in particular, have to be determined by the fine scale data. However, the internal fluxes cancel and, hence, the overall complexity is reduced. The coarse scale sources are computed similarly due to the recursive formulae (3.5). However we have to compute *all* sources on the finest scale. Hence there is no complexity reduction, i.e., we still have the complexity of the reference grid. We will refer to (3.4) and (3.5) as *exact flux and source reconstruction*, respectively.

**Adaptive multiresolution FVS**. According to the subdivision scheme (2.8) the reference scheme (1.3) can be rewritten as

$$\mathbf{v}_L^{n+1} = \sum_{k\in I_0} \mathbf{\Psi}_{0,k,0}^L\, v_{0,k}^{n+1} + \sum_{l=0}^{L-1}\sum_{k\in I_l} \mathbf{\Psi}_{l,k,1}^L\, d_{l,k}^{n+1} \tag{3.6}$$

with the multiscale coefficients determined by (3.2) and(3.3). The idea of the adaptive FVS is to perform the evolution only for *significant* details

$$\mathcal{D}^{n+1} := \Big\{(l,k)\ ;\ |d_{l,k}^{n+1}| > \varepsilon_l,\ k\in I_l,\ l\in\{0,\ldots,L-1\}\Big\}$$

and to discard all other equations. Since this set cannot be computed before the data at time level $t^{n+1}$ are known, a prediction set $\tilde{\mathcal{D}}^{n+1}$ has to be computed from $\mathcal{D}^n$ such that the reliability condition

$$\mathcal{D}^n \cup \mathcal{D}^{n+1} \subset \tilde{\mathcal{D}}^{n+1} \tag{3.7}$$

holds. Then the evolution step of the adaptive scheme consists of the three steps:
**Step 1.** (*Refinement*) Determine the prediction set $\tilde{\mathcal{D}}^{n+1}$ and apply the approximation operator $\mathcal{A}_{\tilde{\mathcal{D}}^{n+1}}$ to the given data, i.e.,

$$\mathbf{v}_{L,\tilde{\mathcal{D}}^{n+1}}^n := \mathcal{A}_{\tilde{\mathcal{D}}^{n+1}}\mathbf{v}_{L,\mathcal{D}^n}^n. \tag{3.8}$$

**Step 2.** (*Evolution*) Evolve the multiscale coefficients corresponding to $\tilde{\mathcal{D}}^{n+1}$ in time according to (3.2), (3.3), i.e.,

$$\mathbf{v}_{L,\tilde{\mathcal{D}}_{n+1}}^{n+1} := \sum_{k\in I_0} \mathbf{\Psi}_{0,k,0}^L v_{0,k}^{n+1} + \sum_{(l,k)\in\tilde{\mathcal{D}}^{n+1}} \mathbf{\Psi}_{l,k,1}^L d_{l,k}^{n+1} = \mathcal{E}_{L,\tilde{\mathcal{D}}^{n+1}}\mathbf{v}_{L,\tilde{\mathcal{D}}^{n+1}}^n, \tag{3.9}$$

**Step 3.** (*Coarsening*) Threshold the new data by applying the approximation operator $\mathcal{A}_\varepsilon$, i.e.,

$$\mathbf{v}_{L,\mathcal{D}^{n+1}}^{n+1} := \mathcal{A}_\varepsilon \mathbf{v}_{L,\tilde{\mathcal{D}}^{n+1}}^{n+1} = \sum_{k\in I_0} \mathbf{\Psi}_{0,k,0}^{L} v_{0,k}^{n+1} + \sum_{(l,k)\in\mathcal{D}^{n+1}} \mathbf{\Psi}_{l,k,1}^{L}\, d_{l,k}^{n+1}. \tag{3.10}$$

We emphasize that all operators are applied locally, i.e., the multiscale operators $\mathcal{M}_L$, $\mathcal{M}_L^{-1}$, the threshold operator $\mathcal{T}_\mathcal{D}$ and the approximation operator $\mathcal{A}_\mathcal{D}$ only work on the set of *significant* coefficients. If there is no inhomogeneity, i.e., $s = 0$, then the complexity of the resulting algorithm might be significantly reduced to the cardinality of $\#\mathcal{D}$. However, if there is a source term and the sources on the local scales are computed by the exact reconstruction strategy (3.5) then the computational complexity is still that of the reference FVS. To some extend this also holds true for the numerical flux computation on local scales using the exact flux reconstruction strategy (3.4). In higher spatial dimensions the cell edges do not coincide on different levels, but a coarse edge is composed of several subedges on finer scales increasing the complexity by some exponential term. Hence the adaptive scheme with both exact flux and source reconstruction is useless for practical purposes. However we will employ it in our analysis of a modified adaptive scheme based on approximate flux and source reconstruction described below. There the modified adaptive scheme is considered as a perturbation of the original adaptive scheme.

**Adaptive grid**. Alternatively to the evolution of the multiscale coefficients we might evolve the cell averages according to (3.1) on a locally refined grid characterized by the index set $\mathcal{G} \subset \{(l,k)\,;\, k \in I_l,\ l = 0,\dots,L\}$, i.e., $\Omega = \bigcup_{(l,k)\in\mathcal{G}} V_{l,k}$ which is computed from $\mathcal{D} = \tilde{\mathcal{D}}^{n+1}$. For this purpose we have to assume that $\mathcal{D}$ is a graded tree of degree $q = 1$, i.e., the relation

$$(l,k) \in \mathcal{D} \Rightarrow (l-1,r) \in \mathcal{D},\ r = \lfloor k/2 \rfloor - q, \dots, \lfloor k/2 \rfloor + q, \tag{3.11}$$

holds for any $l \in \{1,\dots,L-1\}$. Then $\mathcal{G}$ can be determined recursively. For this purpose the index set $\mathcal{G}$ is initialized by all indices of the coarsest discretization. Then, traversing through the levels from coarse to fine we proceed as follows: if $(l,k) \in \mathcal{D}$ then the cell $V_{l,k}$ is locally refined, i.e., the index $(l,k)$ is removed from $\mathcal{G}$ and the indices of the subcells on the finer level are added to $\mathcal{G}$. Finally we obtain the locally adapted grid which naturally corresponds to the leaves of the graded tree of significant details. However, for analytical purposes it is more convenient to write the evolution process in terms of the multiscale coefficients.

**4. Approximate flux and source approximation strategies.** In order to improve the efficiency of the adaptive scheme we present a new strategy how to compute the numerical fluxes and sources on local scales. It is essentially based on polynomial reconstruction techniques as have been introduced in [15]. Then the basic idea is to compute missing data on the finest scale by evaluation of reconstruction polynomials instead of locally performing the inverse multiscale transformation. From a practical point of view, it is sufficient to introduce only the modified fluxes and sources needed to perform the evolution (3.1) of the cell averages corresponding to the adaptive grid $\mathcal{G}$. However, the error analysis relies on the evolution process (3.1), (3.3) of the multiscale coefficients corresponding to the set $\mathcal{D}$. In this case we have to compute additional numerical fluxes and sources. To ensure equivalence of the two evolution processes when applying the inverse MST (2.7) to (3.1), (3.3) we need a consistent computation of the fluxes and sources.

**Polynomial reconstruction**. For each cell $V_{l,k}$ in the adaptive grid, i.e., $(l,k) \in \mathcal{G}$, we compute a *reconstruction polynomial* $R^N_{l,k} \in \Pi_N$ of degree $N$ such that

$$\frac{1}{|V_{l,r}|}\int_{V_{l,r}} R^N_{l,k}(x)\,dx = v^n_{l,r}, \quad \forall r \in \mathcal{S}_{l,k}, \tag{4.1}$$

where $\mathcal{S}_{l,k} \subset I_l$ denotes the reconstruction stencil to be specified below. From these polynomials we can calculate *reconstructed averages*

$$w^n_{L,2^{L-l}k+r} := \frac{1}{|V_{L,2^{L-l}k+r}|}\int_{V_{L,2^{L-l}k+r}} R^N_{l,k}(x)\,dx \tag{4.2}$$

for all cells $V_{L,r} \subset V_{l,k}$, i.e., $r \in \{2^{L-l}k, \dots, 2^{L-l}(k+1)-1\}$. Note that the reconstruction polynomial $R^N_{l,k}$ can be computed by solving the linear system established by the reconstruction conditions (4.1). Alternatively, it can be determined via reconstruction of the primitive function, cf. [15]. For this purpose assume that $\mathcal{S}_{l,k} = \{\underline{k}, \dots, \underline{k}+N\}$ with $k - N \le \underline{k} \le k$. Then determine the interpolation polynomial $Q^{N+1}_{l,k}$ of the primitive function by the interpolation condition

$$Q^{N+1}_{l,k}(x_{l,k'}) = W_{l,k'}, \quad k' \in \{\underline{k}, \dots, \underline{k}+N+1\} \tag{4.3}$$

where $W_{l,k'+1} := W_{l,k'} + h_l v_{l,k'}$, $W_{l,\underline{k}} := h_l \sum_{r<\underline{k}} v_{l,r}$. Finally, the reconstruction polynomial is determined by

$$R^N_{l,k}(x) := \frac{d}{dx} Q^{N+1}_{l,k}(x). \tag{4.4}$$

**Approximate flux reconstruction**. Before describing the new flux computation we need to determine the cell interfaces where we have to compute a numerical flux. For this purpose, we first consider the evolution process (3.1) on the adaptive grid characterized by the index set $\mathcal{G}$. For each cell $V_{l,k}$, $(l,k) \in \mathcal{G}$, the fluxes $F^n_{l,k}$ and $F^n_{l,k+1}$ have to be computed. The union of these interfaces is determined by the set $\overline{\mathcal{F}}_\mathcal{G} := \bigcup_{(l,k)\in\mathcal{G}} \{(l,k),(l,k+1)\}$, for an illustration see Fig. 4.1, interfaces marked by • and ∘. Since $x_{l,k} = x_{l+1,2k}$, we have to avoid inconsistent computations of the fluxes $F_{l,k}$ and $F_{l+1,2k}$. For this purpose, we put $F_{l,k} = F_{l+1,2k}$, i.e., injection from *higher* scales. This procedure is motivated by the derivation of the adaptive scheme according to Section 3. Hence, only at interfaces related to the set

$$\mathcal{F}_\mathcal{G} := \{(l,k) \in \overline{\mathcal{F}}_\mathcal{G} \mid (l+1,2k) \notin \overline{\mathcal{F}}_\mathcal{G}\}$$

the fluxes are calculated from the numerical flux function $F : \mathbb{R}^{2p} \leftrightarrow \mathbb{R}$. In Fig. 4.1 these interfaces are marked by •.

On the other hand, in the evolution process (3.2), (3.3) of the multiscale coefficients we access to the fluxes $F^n_{l,k}$ determined by the set

$$\mathcal{F}_\mathcal{D} := \bigcup_{(l,k)\in\mathcal{D}} \bigcup_{r\in\mathcal{M}^1_{l,k}} \{(l+1,r),(l+1,r+1)\} \cup \bigcup_{k\in I_0} \{(0,k),(0,k+1)\} \supset \overline{\mathcal{F}}_\mathcal{G}.$$

For an illustration see Fig. 4.2, interfaces marked by • and ∘. Since $\mathcal{F}_\mathcal{D} \supset \overline{\mathcal{F}}_\mathcal{G}$, we have to provide the flux computation for all indices $(l,k) \in \mathcal{F}_\mathcal{D}$. Here we have to distinguish three cases: (i) if $(l,k) \in \mathcal{F}_\mathcal{G}$ the flux is computed by the numerical flux function $F$ with respect to the reconstructed averages (4.2), i.e.,

$$\check{F}^n_{l,k} = F(w^n_{L,2^{L-l}k-p}, \dots, w^n_{L,2^{L-l}k+p-1}); \tag{4.5}$$

(ii) if $(l,k) \notin \mathcal{F}_\mathcal{G}$, but there already exists a flux on a higher scale, i.e., $(j, 2^{j-l}k) \in \mathcal{F}_\mathcal{G}$ for one $j \in \{l+1, \dots, L\}$, then we access to this value, i.e., the flux is computed by injection from *above*

$$\check{F}^n_{l,k} = \check{F}^n_{j,2^{j-l}k}; \tag{4.6}$$

(iii) if neither (4.5) nor (4.6) does apply, then there exists $j' = \max\{j \,|\, (j, 2^{j-l}k) \in \mathcal{F}_\mathcal{D}\}$ and the flux is computed by injection from *below*

$$\check{F}^n_{l,k} = \check{F}^n_{j',2^{j'-l}k} = F(w^n_{L,2^{L-j'}k-p}, \dots, w^n_{L,2^{L-j'}k+p-1}). \tag{4.7}$$

In this case the definition of the flux is somewhat arbitrary. In principle, any $j' \geq \max\{j \,|\, (j, 2^{j-l}k)\} \in \mathcal{F}_\mathcal{D}$ is admissible. We only have to make sure that for any interface $x_{l,k} = x_{l+1,2k} = \ldots = x_{L,2^{L-l}k}$ there is a unique value. Note that the third case only becomes effective if $(l,k) \in \mathcal{F}_\mathcal{D} \backslash \overline{\mathcal{F}}_\mathcal{G}$, i.e., when performing the evolution process (3.2), (3.3) for the multiscale coefficients.

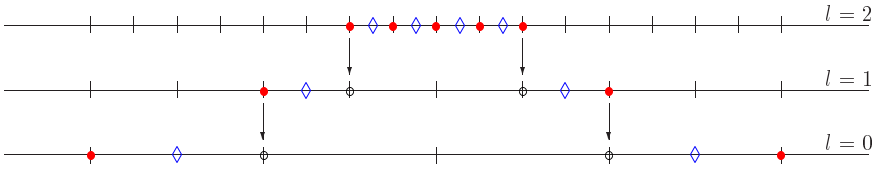


FIG. 4.1. *Evolution process on adaptive grid: $\mathcal{G}$ indicated by cell midpoints ◊, set $\mathcal{F}_\mathcal{G}$ of interfaces ● with flux computation and set $\overline{\mathcal{F}}_\mathcal{G} \backslash \mathcal{F}_\mathcal{G}$ of interfaces ○ with flux computation by injection. Sources have only to be computed for the cells of the adaptive grid determined by $\mathcal{G}$.*

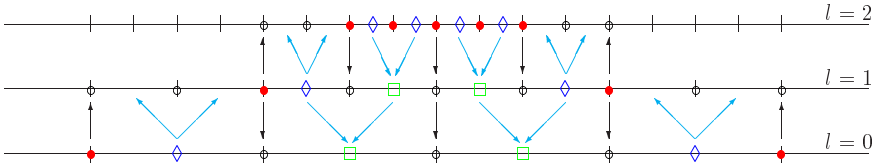


FIG. 4.2. *Evolution process of multiscale coefficients: $\mathcal{G}$ indicated by cell midpoints ◊, set $\mathcal{D}$ of cells with significant details □, set $\mathcal{F}_\mathcal{G}$ of interfaces ● with flux computation and set $\mathcal{F}_\mathcal{D} \backslash \mathcal{F}_\mathcal{G}$ of interfaces ○ with flux computation by injection; here $s = 1$. Sources have not only to be computed for $\mathcal{G}$ but are also accessed for $\mathcal{S}_\mathcal{D} \setminus \mathcal{S}_\mathcal{G}$. The latter are determined by weighted injection.*

**Approximate source reconstruction**. For the source computation we have to avoid the complexity of the reference mesh that is involved in the exact source reconstruction (3.5) due to the definition of the cell averages and the nestedness of the grid hierarchy. To overcome this obstruction we employ some quadrature rule

$$\sum_{i=0}^{m} w_i f(x_i) = \int_{V_{l,k}} f(x)\,dx + E_f(h_l) \tag{4.8}$$

determined by the nodes $x_i \in V_{l,k}$ and the weights $w_i$, $i = 0, \dots, m$, depending on cell $V_{l,k}$. The error $E_f(h_l)$ is assumed to be bounded up to some constant by

$$|E_f(h_l)| \lesssim h_l^{\alpha+1} \sup_{x \in V_{l,k}} |f^{(\alpha)}(x)| \tag{4.9}$$

for some integer $\alpha = \alpha(m) \geq 1$, for instance one can use a Newton-Cotes formula. This quadrature formula is then applied to the sliding average $\mathcal{V}_{l,k}(x)$ of the reconstruction polynomial $R_{l,k}^N$ determined by

$$\mathcal{V}_{l,k}(x) := \frac{1}{h_L} \int_{x-h_L/2}^{x+h_L/2} R_{l,k}^N(z)\, dz = \frac{1}{h_L} \left( Q_{l,k}^{N+1}(x+h_L/2) - Q_{l,k}^{N+1}(x-h_L/2) \right). \tag{4.10}$$

In the course of the evolution process (3.1) on the adaptive grid we then compute the sources for $(l,k) \in \mathcal{G} \equiv \mathcal{S}_\mathcal{G}$ by

$$\check{S}_{l,k}^n = \frac{1}{h_l} \sum_{i=0}^{m} w_i\, S(\mathcal{V}_{l,k}(x_i)). \tag{4.11}$$

In the evolution process (3.2), (3.3) of the multiscale coefficients, see Fig. 4.2, we access to the following sources

$$\mathcal{S}_\mathcal{D} = \bigcup_{(l,k)\in\mathcal{D}} \bigcup_{r\in\mathcal{M}_{l,k}^1} \{(l+1,r)\} \cup \bigcup_{k\in I_0} \{(0,k)\} \supset \mathcal{S}_\mathcal{G}.$$

Inconsistent computation of sources $S_{l-1,\lfloor k/2 \rfloor}$, $S_{l,k}$ and $S_{l+1,2k}$, $S_{l+1,2k+1}$ on different levels has to be avoided. For this purpose, we distinguish between two cases: If there already exist sources on higher scales, i.e., $(j, 2^{j-l}k) \in \mathcal{S}_\mathcal{D}$ for a $j \in \{l+1, \ldots, L\}$, then we access to these values. Since we are now dealing with averages instead of point values we have to average these values, i.e.,

$$\check{S}_{l,k}^n = 2^{l-j} \sum_{i=0}^{2^{j-l}-1} \check{S}_{j,2^{j-l}k+i}^n. \tag{4.12}$$

Finally, if neither (4.11) nor (4.12) does apply, then there exists $j \in \{0, \ldots, l-1\}$ such that $(j, \lfloor k/2^{l-j} \rfloor) \in \mathcal{G}$. In this case the source is computed by injection from *below* and the exact source reconstruction (3.5)

$$\check{S}_{l,k}^n = \check{S}_{j,\lfloor k/2^{l-j} \rfloor}^n - \bar{S}_{j,\lfloor k/2^{l-j} \rfloor}^n + \bar{S}_{l,k}. \tag{4.13}$$

Note that this case is only applied for evolving the multiscale coefficients. In practice, the cell averages corresponding to the adaptive grid are evolved. We only need this case for analytical purposes. Note also that we are somewhat free in the definition of $\check{S}_{l,k}^n$ in this case. We only have to satisfy the constraint

$$2^{j-l} \sum_{i=0}^{2^{l-j}-1} \check{S}_{l,2^{l-j}\lfloor k/2^{l-j} \rfloor + i}^n = \check{S}_{j,\lfloor k/2^{l-j} \rfloor}^n.$$

Obviously, this condition holds true for our definition as can be concluded from (3.5).

**Equivalence of evolution step**. From Fig. 4.1 and 4.2 we conclude that $\mathcal{F}_\mathcal{G} \subset \overline{\mathcal{F}}_\mathcal{G} \subset \mathcal{F}_\mathcal{D}$ and $\mathcal{S}_\mathcal{G} \subset \mathcal{S}_\mathcal{D}$, respectively. We have to ensure that the evolution equation (3.1) of the cell averages are identical to the evolution equations (3.2), (3.3) to which we apply the inverse MST (2.7). In case of the exact flux and source reconstruction the equivalence is obvious, because all fluxes and sources are computed on the finest level. To ensure the equivalence in case of approximate flux and source reconstruction

some fluxes in $\mathcal{F}_\mathcal{D}$ are not calculated from the numerical flux function or taken from higher scales, see "↓" in Fig. 4.1, but from lower scales, see "↑" in Fig. 4.2. Similarly, we note that some sources in $\mathcal{S}_\mathcal{D}$ are not calculated from the numerical source function or taken from higher scales, see " ↘ " and " ↙ " in Fig. 4.2, but from lower scales, see " ↖ " and " ↗ " in Fig. 4.2.

PROPOSITION 4.1. *The approximate flux and source reconstruction strategy (4.5), (4.6), (4.7) and (4.11), (4.12), (4.13) ensure equivalence of the evolution steps (3.1) and (3.2), (3.3)), respectively.*

*Proof.* To prove this equivalence we confine ourselves without loss of generality to the situation sketched in Fig. 4.3. The data of the adaptive grid, here $v_{l+1,2k+i}$, $i = 0, 1$, are evolved according to (3.1)

$$v^{n+1}_{l+1,2k+i} = v^n_{l+1,2k+i} - \frac{\tau}{h_{l+1}}(F^n_{l+1,2k+i+1} - F^n_{l+1,2k+i}) + \tau\,\bar{S}^n_{l+1,2k+i}, \quad i = 0, 1. \tag{4.14}$$

Alternatively, we evolve $v_{l,r}$, $r \in \mathcal{G}^0_{l,2k+i}$ and $d_{l,r}$, $r \in \mathcal{G}^1_{l,2k+i}$ according to (3.2), (3.3)

$$\begin{aligned} v^{n+1}_{l,r} &= v^n_{l,r} - \frac{\tau}{h_l}\left(F^n_{l,r+1} - F^n_{l,r}\right) + \tau\bar{S}^n_{l,r} \\ &= v^n_{l,r} - \frac{\tau}{h_{l+1}} \sum_{s\in\mathcal{M}^0_{l,r}} m^{l,0}_{s,r}(F^n_{l+1,s+1} - F^n_{l+1,s}) + \tau \sum_{s\in\mathcal{M}^0_{l,r}} m^{l,0}_{s,r}\bar{S}^n_{l+1,s}, \end{aligned} \tag{4.15}$$

$$d^{n+1}_{l,r} = d^n_{l,r} - \frac{\tau}{h_{l+1}} \sum_{s\in\mathcal{M}^1_{l,r}} m^{l,1}_{s,r}(F^n_{l+1,s+1} - F^n_{l+1,s}) + \tau \sum_{s\in\mathcal{M}^1_{l,r}} m^{l,1}_{s,r}\bar{S}^n_{l+1,s}. \tag{4.16}$$

We then verify that applying the inverse MST (2.7) to (4.15) and (4.16) results in (4.14). This follows immediately from the reversibility of the multiscale decomposition. ∎

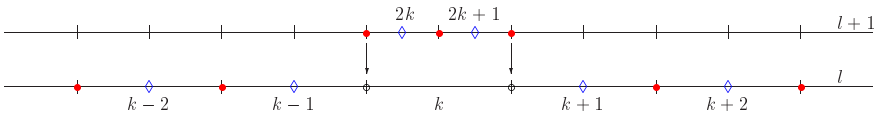


FIG. 4.3. *Evolution on adaptive grid $\mathcal{G}$ indicated by cell midpoints ◊, set $\mathcal{F}_\mathcal{G}$ of interfaces ● with flux computation and set $\overline{\mathcal{F}}_\mathcal{G}\backslash\mathcal{F}_\mathcal{G}$ of interfaces ○ with flux computation by injection.*

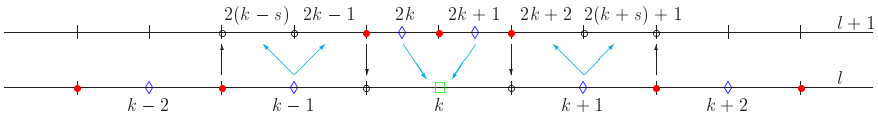


FIG. 4.4. *Evolution on tree $\mathcal{D}$ of cells with significant details □ and coarse scale cells, adaptive grid $\mathcal{G}$ indicated by cell midpoints ◊, set $\mathcal{F}_\mathcal{G}$ of interfaces ● with flux computation and set $\mathcal{F}_\mathcal{D}\backslash\mathcal{F}_\mathcal{G}$ of interfaces ○ with flux computation by injection; here $s = 1$.*

**5. Error analysis.** The objective of the proposed adaptive scheme is to reduce for a given FVS computational cost and memory requirements while preserving the accuracy of the reference scheme. Hence, the error has to be considered for data on the reference mesh rather than on the adaptive grid. To prolongate the data from the adaptive grid to the reference grid we employ the multiscale representation (2.10)

where we put the non-significant details to zero. In order to quantify the error we introduce the averages $\hat{\mathbf{u}}_L^n$ of the exact solution, the averages $\mathbf{v}_L^n$ determined by the FVS and the prolongated averages $\overline{\mathbf{v}}_L^n$ of the adaptive scheme.

An ideal strategy would be to prescribe an error tolerance *tol*. Then the number of refinement levels $L$ should be determined during the computation such that the error meets the tolerance, i.e.,

$$\|\hat{\mathbf{u}}_L^n - \overline{\mathbf{v}}_L^n\| \leq tol$$

for possibly small $L$. Here $\|\cdot\|$ denotes an appropriate norm to be specified below. Since no error estimator is available for the adaptive scheme, we split the error into two parts corresponding to the *discretization error* $\boldsymbol{\tau}_L^n := \hat{\mathbf{u}}_L^n - \mathbf{v}_L^n$ of the reference FVS and the *perturbation error* $\mathbf{e}_L^n := \mathbf{v}_L^n - \overline{\mathbf{v}}_L^n$, i.e.,

$$\|\hat{\mathbf{u}}_L^n - \overline{\mathbf{v}}_L^n\| \leq \|\boldsymbol{\tau}_L^n\| + \|\mathbf{e}_L^n\| \leq tol. \tag{5.1}$$

We now assume that there is an a priori error estimate of the discretization error, i.e., $\boldsymbol{\tau}_L^n \sim h_L^\alpha$ where $h_L$ denotes the spatial step size and $\alpha$ the order of convergence. Then we ideally would determine the number of refinement levels $L$ such that $h_L^\alpha \sim tol$. In order to preserve the accuracy of the reference FVS we now may admit a perturbation error which is proportional to the discretization error, i.e., $\|\mathbf{e}_L^n\| \sim \|\boldsymbol{\tau}_L^n\|$. From this we conclude

$$L = L(tol, \alpha) \quad \text{and} \quad \varepsilon = \varepsilon(L). \tag{5.2}$$

Therefore it remains to verify that the perturbation error can be controlled. Note, that in each time step we introduce an error due to the threshold procedure. Obviously, this error accumulates in each step, i.e., the best we can hope for is an estimate of the form

$$\|\mathbf{e}_L^n\| \leq C\, n\, \varepsilon.$$

However, the threshold error may be amplified in addition by the evolution step. In order to control the cumulative perturbation error we have to prove that the constant $C$ is independent of $L$, $n$, $\tau$ and $\varepsilon$. For this purpose we will consider the following issues in more detail, namely, (i) the uniform boundedness of the perturbation error, (ii) the reliability of the prediction procedure and (iii) the error of the approximate flux and source reconstruction.

**5.1. Perturbation error.** In a first step we verify the uniform boundedness of the perturbation error between the reference FVS and the adaptive MR-FVS in the weighted $l_1$-metric $\|\mathbf{v}_L\| := h_L \sum_{k \in I_L} |v_{L,k}|$ on the reference grid. This metric is equal to the $L_1$-norm of a piecewise constant function. Since the schemes are defined on the real axis in order to avoid boundary conditions, the set $I_L$ is countable. To ensure boundedness of the weighted $L^1$-norm we therefore will always confine ourselves to an arbitrary but fixed compact set $[a, b]$ and $I_L$ is chosen such that $\cup_{k \in I_L} V_{L,k} \subseteq [a, b]$ with $N_L := \#I_L < \infty$. Due to dyadic grid refinement we have $N_l = 2N_{l-1} = 2^l N_0$ and $h_l = 2h_{l+1} = 2^{L-l} h_L$, respectively. Confining ourselves to a compact set is justified by considering compactly supported initial data $u_0$. Then by the finite speed of propagation the solution is compactly supported too. Moreover, convergence of the reference scheme is typically verified in the $L^1_{loc}$-norm.

In order to investigate the perturbation error we introduce the evolution operators $\mathcal{E}_L$ of the reference FVS and $\bar{\mathcal{E}}_{L,\mathcal{D}}$, $\check{\mathcal{E}}_{L,\mathcal{D}}$ of the adaptive MR-FVS corresponding to the

adaptive grid $\mathcal{G}(\mathcal{D})$ with exact and approximate flux and source reconstruction, respectively. These are determined by (3.6) and (3.9). Note that for analytical purposes it is convenient to consider the evolution operators in the multiscale representation (2.8). Then the schemes can be represented in operator form as $\mathbf{v}_L^{n+1} = \mathcal{E}_L \mathbf{v}_L^n$ (reference FVS), $\overline{\mathbf{v}}_L^{n+1} = \mathcal{A}_\varepsilon \bar{\mathcal{E}}_{L,\tilde{\mathcal{D}}^{n+1}} \mathcal{A}_{\tilde{\mathcal{D}}^{n+1}} \overline{\mathbf{v}}_L^n$ (adaptive MR-FVS with exact reconstruction) and $\check{\mathbf{v}}_L^{n+1} = \mathcal{A}_\varepsilon \check{\mathcal{E}}_{L,\tilde{\mathcal{D}}^{n+1}} \mathcal{A}_{\tilde{\mathcal{D}}^{n+1}} \check{\mathbf{v}}_L^n$ (adaptive MR-FVS with approximate reconstruction).

Comparing the evolution operators of the reference scheme and the adaptive scheme with exact flux and source reconstruction we conclude that the latter can be interpreted as the reference scheme to which we apply the approximation operator $\mathcal{A}_{\tilde{\mathcal{D}}^{n+1}}$, i.e.,

$$\bar{\mathcal{E}}_{L,\tilde{\mathcal{D}}^{n+1}} \mathcal{A}_{\tilde{\mathcal{D}}^{n+1}} \overline{\mathbf{v}}_L^n = \mathcal{A}_{\tilde{\mathcal{D}}^{n+1}} \mathcal{E}_L \overline{\mathbf{v}}_L^n \tag{5.3}$$

provided that $\overline{\mathbf{v}}_L^n$ is the result of the adaptive scheme based on exact flux reconstruction, i.e., $\mathcal{A}_{\tilde{\mathcal{D}}^{n+1}} \overline{\mathbf{v}}_L^n = \mathcal{A}_\varepsilon \overline{\mathbf{v}}_L^n = \overline{\mathbf{v}}_L^n$ and $\mathcal{D}^n \subset \tilde{\mathcal{D}}^{n+1}$. Now we can estimate the perturbation error.

THEOREM 5.1. *(Uniform boundedness of perturbation error) Let the following assumptions hold true:*

*(A1) the approximation error is uniformly bounded, i.e.,* $\|\mathbf{u}_L - \mathcal{A}_\varepsilon \mathbf{u}_L\| \le C_1 \varepsilon$;

*(A2) flux and source reconstruction is accuracy preserving, i.e.,*

$$\|\overline{\mathcal{E}}_{L,\tilde{\mathcal{D}}^{n+1}} \mathcal{A}_{\tilde{\mathcal{D}}^{n+1}} \check{\mathbf{v}}_L^n - \check{\mathcal{E}}_{L,\tilde{\mathcal{D}}^{n+1}} \mathcal{A}_{\tilde{\mathcal{D}}^{n+1}} \check{\mathbf{v}}_L^n\| \le C_2 \varepsilon;$$

*(A3) the reference FVS is essentially $l_1$-contractive, i.e.,*

$$\|\mathcal{E}_L \mathbf{u}_L - \mathcal{E}_L \mathbf{v}_L\| \le (1 + C_3 \tau) \|\mathbf{u}_L - \mathbf{v}_L\|;$$

*(A4) the prediction is reliable in the sense of* (3.7)*, i.e.,*$\|\mathcal{A}_{\tilde{\mathcal{D}}^{n+1}} \mathcal{E}_L \check{\mathbf{v}}_L^n - \mathcal{E}_L \check{\mathbf{v}}_L^n\| \le C_4 \varepsilon$;

*(A5) the initial data are consistent, i.e.,* $\|\mathbf{v}_L^0 - \check{\mathbf{v}}_L^0\| \le C_5 \varepsilon$.

*Then the perturbation error is bounded by*

$$\|\mathbf{e}_L^n\| = \|\mathbf{v}_L^n - \check{\mathbf{v}}_L^n\| \le C \frac{\varepsilon}{\tau} \tag{5.4}$$

*for $n\tau \le T$ where $C$ is independent of $L$, $n$, $\tau$ and $\varepsilon$.*

*Proof.* In a first step we split the perturbation error into its different contributions corresponding to the contraction of the reference FVS (A3), the reliability of prediction, the error of the flux reconstruction (A2) and the threshold error (A1), i.e.,

$$\|\mathbf{e}_L^n\| \le \|\mathcal{E}_L \mathbf{v}_L^{n-1} - \mathcal{E}_L \check{\mathbf{v}}_L^{n-1}\| + a_{n-1} + b_{n-1} + c_{n-1}$$

with

$$a_{n-1} := \|\mathcal{E}_L \check{\mathbf{v}}_L^{n-1} - \mathcal{A}_{\tilde{\mathcal{D}}^n} \mathcal{E}_L \check{\mathbf{v}}_L^{n-1}\|, \quad b_{n-1} := \|\bar{\mathcal{E}}_{L,\tilde{\mathcal{D}}^n} \mathcal{A}_{\tilde{\mathcal{D}}^n} \check{\mathbf{v}}_L^{n-1} - \check{\mathcal{E}}_{L,\tilde{\mathcal{D}}^n} \mathcal{A}_{\tilde{\mathcal{D}}^n} \check{\mathbf{v}}_L^{n-1}\|,$$
$$c_{n-1} := \|\check{\mathcal{E}}_{L,\tilde{\mathcal{D}}^n} \mathcal{A}_{\tilde{\mathcal{D}}^n} \check{\mathbf{v}}_L^{n-1} - \mathcal{A}_\varepsilon \check{\mathcal{E}}_{L,\tilde{\mathcal{D}}^n} \mathcal{A}_{\tilde{\mathcal{D}}^n} \check{\mathbf{v}}_L^{n-1}\|.$$

Here we use (5.3), i.e., the adaptive scheme with exact flux and source reconstruction can be interpreted as the reference scheme to which we apply the approximation operator. This is admissible because $\mathcal{A}_\varepsilon \check{\mathbf{v}}_L^{n-1} = \check{\mathbf{v}}_L^{n-1}$ according to the definition of the adaptive scheme.

Then the first term is estimated by the contraction property of the reference scheme (A3); the second term by the approximation property (A4), where we assume that the prediction strategy is reliable; the third term by the accuracy preserving

property (A2) of the flux reconstruction and the fourth term by the approximation property (A1). Hence the perturbation error can be further estimated by

$$\|\mathbf{e}_L^n\| \leq \|\mathbf{e}_L^{n-1}\| \, (1 + C_3 \, \tau) + (C_1 + C_2 + C_4) \, \varepsilon.$$

By recursion we obtain further

$$\|\mathbf{e}_L^n\| \leq \|\mathbf{e}_L^0\| \, (1 + C_3 \, \tau)^n + \varepsilon \, (C_1 + C_2 + C_4) \, \sum_{i=0}^{n-1} (1 + C_3 \, \tau)^i.$$

Setting $\overline{C} := \max(C_1 + C_2, C_5)$ we finally conclude

$$\|\mathbf{e}_L^n\| \leq \varepsilon \, \overline{C} \, \frac{(1 + C_3 \, \tau)^{n+1} - 1}{C_3 \, \tau} \leq \varepsilon \, \overline{C} \, \frac{e^{C_3 \, (n+1) \, \tau} - 1}{C_3 \, \tau}$$

in case of $C_3 \neq 0$ and

$$\|\mathbf{e}_L^n\| \leq \varepsilon \, \overline{C} \, \frac{(n+1) \, \tau}{\tau}$$

if the FVS is $l^1$–contractive, i.e., $C_3 = 0$. Since the maximal number of time steps is bounded by $n \leq T/\tau$ for a bounded time interval $[0, T]$, $T < \infty$, the assertion follows. □

A similar result has been proven for the adaptive MR-FVS with *exact* flux reconstruction, cf. [18] (Theorem 5, p. 91) or [9]. Here the original MR-FVS is only used as an intermediate value, i.e., in each time step the data of the modified MR-FVS scheme are used instead of the data of the original MR-FVS from the previous time step. One might introduce the adaptive scheme with exact flux approximation where the time evolution is always performed on its own data, i.e., $\bar{\mathbf{v}}_L^n = \mathcal{A}_\varepsilon \bar{\mathcal{E}}_{L,\tilde{\mathcal{D}}^n} \mathcal{A}_{\tilde{\mathcal{D}}^n} \bar{\mathbf{v}}^{n-1}$, where $\tilde{\mathcal{D}}^n = \tilde{\mathcal{D}}^n(\bar{\mathbf{v}}_L^{n-1})$. Then in the proof of Theorem 5.1 the prediction sets for $\overline{\mathbf{v}}_L^n$ and $\check{\mathbf{v}}_L^n$ would be different because $\tilde{\mathcal{D}}^n(\overline{\mathbf{v}}_L^{n-1}) \neq \tilde{\mathcal{D}}^n(\check{\mathbf{v}}_L^{n-1})$.

From Theorem 5.1 and (5.1) we immediately conclude that the accuracy of the reference FVS is preserved provided that $\varepsilon$ is chosen sufficiently small.

COROLLARY 5.2. *(Choice of threshold parameter) If the discretization error of the reference FVS is bounded by* $\|\hat{\mathbf{u}}_L^n - \mathbf{v}_L^n\|_{1,L} \leq C \, 2^{-\alpha \, L}$ *for some* $\alpha > 0$*, then the accuracy is preserved by the adaptive scheme provided that* $\varepsilon \sim 2^{-(1+\alpha) \, L}$ *and the time step* $\tau$ *is limited by a CFL constraint.*

The usefulness of Theorem 5.1 crucially depends on the verification of the assumptions (A1) — (A5). The convergence of the subdivision scheme implies the boundedness of the approximation error in the weighted $l_1$-metric. This follows by Theorem 2.1. Furthermore, for scalar conservation laws in 1D there exist (essentially) $l^1$–contractive schemes, cf. [11]. Concerning the consistent discretization of the initial data a natural choice is given by the approximation operator, i.e., $\check{\mathbf{v}}_L^0 := \mathcal{A}_{\boldsymbol{\varepsilon}} \mathbf{v}_L^0$. It remains to verify (i) the reliability condition for the evolution of the adaptive MR-FVS with *exact* reconstruction and (ii) the boundedness of the error between time evolution using exact and approximate reconstruction, respectively. These issues will be addressed in the following two sections.

**5.2. Reliability of Prediction.** In [9] the reliability condition (3.7) was verified for the adaptive MR-FVS with *exact* flux reconstruction in case of a *homogeneous* conservation law for a special prediction strategy to be summarized below. It needs

to be slightly modified to take into account source terms via *exact* source reconstruction. In addition, we have to consider that in each time step the original adaptive MR-FVS is applied to the data of the modified MR-FVS with approximate flux and source reconstruction. For this purpose we first have to describe the prediction strategy developed in [9], see Sec. 5.2.1. Then we have to verify the $l^\infty$-stability of the modified adaptive MR-FVS with approximate reconstruction, see Sec. 5.2.2. Finally we can prove the reliability condition for the original adaptive MR-FVS with exact reconstruction applied to the data of the modified scheme, see Sec. 5.2.3.

**5.2.1. Prediction strategy.** For simplicity of representation we introduce the convention $d_{l,k,0} \equiv v_{l,k}$ and $d_{l,k,1} \equiv d_{l,k}$ for the averages and the details, respectively. The basic idea is to determine all coefficients $d^{n+1}_{l',k',e'}$, $e' \in E$, on the new time level which are influenced by a coefficient $d^n_{l,k,e}$, $e \in E$, on the old time level. This set is referred to as the influence set $\mathcal{D}_{l,k,e}$. Then we are nesting the coefficients $d^n_{l,k,e}$ given at the old time level and finally determine the prediction set $\tilde{\mathcal{D}}^{n+1}$.

**Influence set**. To determine the set $\mathcal{D}_{l,k,e}$ we first have to compute the *range of influence* $\Sigma_{l,k,e}$ of the coefficient $d^n_{l,k,e}$ and the *domain of dependence* $\tilde{\Sigma}_{l',k',e'}$ of the coefficient $d^{n+1}_{l',k',e'}$. In the range of influence we collect all averages $v^n_{L,r}$, that are influenced by the detail $d^n_{l,k,e}$ whereas the domain of dependence contains all averages $v^{n+1}_{L,r}$ on which the coefficient $d^{n+1}_{l',k',e'}$ depends. According to the setting in Sec. 2 these sets turn out to be

$$\begin{aligned}
\tilde{\Sigma}_{l,k,0} &= \{2^{L-l}k, \dots, 2^{L-l}(k+1)-1\} = \Sigma_{l,k,1},\\
\Sigma_{l,k,0} &= \{2^{L-l}(k-2s)+2s, \dots, 2^{L-l}(k+2s+1)-(2s+1)\},\\
\tilde{\Sigma}_{l,k,1} &= \{2^{L-l}(k-s), \dots, 2^{L-l}(k+s+1)-1\}.
\end{aligned} \tag{5.5}$$

Note that the index sets $\tilde{\Sigma}_{l',k',e'} \subset I_L$ and $\Sigma_{l,k,e} \subset I_L$ correspond to data on the reference mesh but for different time level $n+1$ and $n$, respectively. By the evolution process (3.9) with exact reconstruction (3.4) and (3.5) the domain of dependence has to be extended taking into account the stencil of numerical flux $F$ and source $S$ determined by (1.4) and (1.5), respectively, i.e.,

$$\tilde{\Sigma}^-_{l',k',e'} := \bigcup_{r \in \tilde{\Sigma}_{l',k',e'}} \{r-p, \dots, r+p\}. \tag{5.6}$$

Then the influence set is determined by

$$\mathcal{D}_{l,k,e} = \{(l',k',e') \in \mathcal{D} \ ; \ \tilde{\Sigma}^-_{l',k',e'} \cap \Sigma_{l,k,e} \neq \emptyset\}.$$

**Nesting of coefficients**. The prediction strategy has to take into account that the coefficients $d^n_{l,k,e}$ may not only cause a perturbation in the neighborhood of the cell $V_{l,k}$ because of the time evolution but may also influence coefficients $d^{n+1}_{l',k',e'}$ on higher scales, where $l' > l+1$ is admissible. Since the additional higher levels inflate the influence set, we would like to bound the number of higher levels to a minimum number. For this purpose we introduce the nesting of details where we fix some $\sigma > 1$ and assign to each coefficient corresponding to $(l,k,e) \in \mathcal{D}^n$ a unique index $\nu = \nu(l,k,e)$ such that

$$2^{\nu(l,k,e)\,\sigma}\,\varepsilon_l < |d^n_{l,k,e}| \leq 2^{(\nu(l,k,e)+1)\,\sigma}\,\varepsilon_l. \tag{5.7}$$

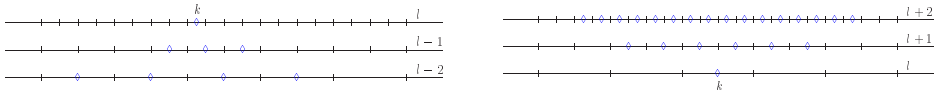


FIG. 5.1. *Illustration of the range of influence (left) and the range of dependence (right) for a significant detail* $(l,k) \in \mathcal{D}$ *indicated by the cell midpoints* ◊ *with grading parameter* $q = 1$.

We will see later on that the parameter $\sigma$ is linked to the smoothness of the primal wavelet functions, see Theorem 2.1. Since the index $\nu(l,k,e)$ becomes the smaller the larger $\sigma$ is, it is convenient to choose $\sigma$ as large as possible.

**Prediction set**. From the influence set $\mathcal{D}_{l,k,e}$ and the nesting of coefficients we determine the prediction set

$$\tilde{\mathcal{D}}^{n+1} := \mathcal{D}^n \cup \bigcup_{(l,k,e)\in\overline{\mathcal{D}}^n} \{(l',k',e') \in \mathcal{D}_{l,k,e} \ ; \ l' \le l + \nu(l,k,e)\} \tag{5.8}$$

with $\overline{\mathcal{D}}^n := \mathcal{D}^n \cup \{(0,k,0) \ ; \ k \in I_0\}$. For computational but also analytical purposes we inflate this set additionally where we apply the grading procedure (3.11). For instance, the grading ensures that the local multiscale transformation (2.3), (2.6) and (2.7), respectively, can be realized by *one* sweep through the refinement levels provided the grading parameter $q$ is chosen such that $q \ge s$, see [18], p. 36. By the grading procedure a significant detail $(l,k) \in \mathcal{D}$ will cause all details on lower scales $j = l-1,\dots,1$ in the range of influence $\Sigma_{l,k}^{G,(j)} \subset I_j$ to be put significant independent of their value. On the other hand, for all non-significant details $(l,k) \notin \mathcal{D}$ the grading ensures that all details on higher scales $j = l+1,\dots,L-1$ in the range of influence $\tilde{\Sigma}_{l,k}^{G,(j)} \subset I_j$ can not be significant otherwise $(l,k) \in \mathcal{D}$. According to our setting in Sec. 2 the range of influence and dependence, respectively, can be estimated by

$$\begin{aligned}
\bar{\Sigma}_{l,k}^{G,(j)} &\subset \{\lfloor k/2^{l-j} \rfloor - 2^{l-j-1}q, \dots, \lfloor k/2^{l-j} \rfloor + 2^{l-j-1}q\},\\
\tilde{\Sigma}_{l,k}^{G,(j)} &\subset \{2^{j-l}(k-q) - (2^{j-l}-2)q, \dots, 2^{j-l}(k+q) + (2^{j-l}-2)q + 2^{j-l} - 1\}.
\end{aligned}$$

Note that the grading will inflate the prediction set but does not deteriorate the overall complexity.

**5.2.2. $l^\infty$-stability of modified adaptive MR-FVS.** To prove reliability of the prediction set $\tilde{\mathcal{D}}^{n+1}$ of the original MR-FVS determined by the data $\check{\mathbf{v}}_L^n$ of the modified MR-FVS we have to verify that $\check{\mathbf{v}}_L^n$ is uniformly bounded in the sup-norm. Therefore we need the reliability of $\tilde{\mathcal{D}}^\nu$, $\nu = 0,\dots,n$. This recursive proof is initialized by the proper computation of the initial data such that $\tilde{\mathcal{D}}^0 = \mathcal{D}^0$. We emphasize that in the course of the recursion all constants have to be uniform, i.e., they do not depend on $L$, $n$, $\tau$ and $\varepsilon$, respectively.

LEMMA 5.3. *(Boundedness of adaptive FVS in sup–norm) Assume that the following conditions hold true:*

*(A6) the subdivision scheme converges uniformly in the sup–norm;*

*(A8) the reference FVS is stable in* $l^\infty$*, i.e.,* $\|\mathcal{E}_L\,\mathbf{v}_L\|_{l^\infty} \le (1 + C\,\tau)\,\|\mathbf{v}_L\|_{l^\infty}$;

*(A9) the error of the initial data approximation can be estimated by*

$$\|\check{\mathbf{v}}_L^0 - \mathbf{v}_L^0\|_{l^\infty} \le C\,\varepsilon/\tau \ \text{ and } \ \|\mathbf{v}_L^0 - \hat{\mathbf{u}}_L^0\|_{l^\infty} \le C\,\varepsilon/\tau,$$

*where* $\hat{\mathbf{u}}_L^0$ *denotes the averages of the initial data;*

*(A10) the threshold values are determined by* $\varepsilon_j = 2^{j-L}\,\varepsilon$ *with* $\varepsilon \sim 2^{-(1+\alpha)L}$ *for some* $\alpha > 0$*;*

*(A11) the CFL condition holds on the finest resolution level, i.e.,* $\tau \sim 2^{-L}$.
*Then the approximation* $\check{\mathbf{v}}_L^n$ *corresponding to the adaptive FVS with approximate flux reconstruction is uniformly bounded in the sup–norm, i.e.,*

$$\|\check{\mathbf{v}}_L^n\|_{l^\infty} \le C(T, u_0) \qquad \text{for} \quad n\,\tau \le T, \tag{5.9}$$

*provided that the prediction set* $\tilde{\mathcal{D}}^\nu$ *satisfies the reliability property (3.7) and the error of the approximate flux and source reconstruction is bounded, i.e.,*
*(A7)* $\|\check{\mathcal{E}}_{L,\tilde{\mathcal{D}}^\nu}\,\mathcal{A}_{\tilde{\mathcal{D}}^\nu}\,\check{\mathbf{v}}_L^{\nu-1} - \bar{\mathcal{E}}_{L,\tilde{\mathcal{D}}^\nu}\,\mathcal{A}_{\tilde{\mathcal{D}}^\nu}\,\check{\mathbf{v}}_L^{\nu-1}\|_{l^\infty} \le C\varepsilon$
*for all previous time steps* $0 \le \nu \le n$.

*Sketch of proof.* A similar result has been proven for the original adaptive MR-FVS with *exact* flux reconstruction, cf. [18] (Lemma 8, p. 102) or [9]. However, the splitting of the error has to be modified taking into account the additional error between exact and approximate flux and source reconstruction. Hence, we start from

$$\begin{aligned}\|\check{\mathbf{v}}_L^n\|_{l^\infty} \le & \|\mathcal{A}_\varepsilon\,\check{\mathcal{E}}_{L,\bar{\mathcal{D}}^n}\,\mathbf{w}_L^{n-1} - \check{\mathcal{E}}_{L,\bar{\mathcal{D}}^n}\,\mathbf{w}_L^{n-1}\|_{l^\infty} + \|\check{\mathcal{E}}_{L,\bar{\mathcal{D}}^n}\,\mathbf{w}_L^{n-1} - \bar{\mathcal{E}}_{L,\bar{\mathcal{D}}^n}\,\mathbf{w}_L^{n-1}\|_{l^\infty} + \\ & \|\bar{\mathcal{E}}_{L,\bar{\mathcal{D}}^n}\,\mathbf{w}_L^{n-1} - \mathcal{E}_L\,\check{\mathbf{v}}_L^{n-1}\|_{l^\infty} + \|\mathcal{E}_L\check{\mathbf{v}}_L^{n-1}\|_{l^\infty}\end{aligned}$$

with $\mathbf{w}_L^{n-1} := \mathcal{A}_{\bar{\mathcal{D}}^n}\check{\mathbf{v}}_L^{n-1}$. The terms of the right-hand side can be estimated by the assumptions and Theorem 2.1 resulting in

$$\|\check{\mathbf{v}}_L^n\|_{l^\infty} \le (1 + C\,\tau)\,\|\check{\mathbf{v}}_L^{n-1}\|_{l^\infty} + \bar{C}\varepsilon.$$

Then the assertion follows by a discrete Cronwall inequality and assumption (A9) on the approximation of the initial data. The details are given in Appendix 7.1. □

Note that an (essentially) $l_1-$ contractive and $l^\infty$-stable scheme, see (A3) in Theorem 5.1 and (A8) in Lemma 5.3, is known to converge to a weak solution of the initial value problem (1.1), (1.2), cf. [11].

**5.2.3. Reliability.** Finally we can prove the reliability condition for the original adaptive MR-FVS with exact reconstruction applied to the data of the modified scheme and, hence, assumption (A4) in Theorem 5.1. The proof is similar to the one presented in [9], [18] in case of a *homogeneous* conservation law. We therefore will omit the details of the proof but will summarize the main steps which are needed later on in Sec. 5.3. Starting point is the observation that we can confine ourselves to the evolution equations on the reference mesh because of the identity (5.3) and the details can be rewritten in terms of finite differences of order $M$ (number of vanishing moments)

$$\Delta_K^M\,u_{L,k} := \sum_{i=0}^{M}(-1)^i\binom{M}{i}u_{L,k+iK} \tag{5.10}$$

with stencil

$$S(M,K,k) := \{k + iK \;:\; i = 0,\dots M\} \subset I_L, \tag{5.11}$$

cf. [9], [18], Lemma 7, p. 99. Then the details can be estimated by

LEMMA 5.4. *(Estimate of details by finite differences) Let $k \in \mathbf{Z}$, $l \in \{0, \dots, L-1\}$ and $K := 2^{L-l-1}$. Furthermore, let $M$ denote the number of vanishing moments of the modified box wavelet. Then the details $d_{l,k}$ can be estimated by*

$$|d_{l,k}| \leq C \sup\{|\Delta_K^M u_{L,r}| \ ; \ r \in I_L \ \text{ s. t. } S(M,K,r) \subset \tilde{\Sigma}_{l,k,1}\}, \tag{5.12}$$

*where the constant $C$ is independent of $l$ and $k$.*
For a proof see [18], Proposition 4, p. 101.

Due to the evolution equation the finite difference operator is also applied to the numerical flux balances and sources, respectively. These can be considered as composite functions $G := g \circ u$. The derivatives of the composite function $G$ can be written in a series of derivatives of $g$ and $u$, respectively, successively applying the chain rule. Then the main idea is to derive a discrete counterpart by which finite differences of the nonlinear function $G$ are estimated by finite differences of the averages. For this purpose, the following assumption has to hold for $G$:

ASSUMPTION 1. *Let $D \subset \mathbb{R}^{\overline{p}}$ be a bounded domain of admissible states. Then the nonlinear function $G : \mathbb{R}^{\overline{p}} \longmapsto \mathbb{R}$ is assumed to be regular in the following sense:*

1. *$G$ is piecewise smooth, i.e., there are open subsets $D_i \subset D$, $i = 1, \dots, K$, with $D = \bigcup_{i=1}^{K} \overline{D}_i$, such that $G \in C^R(D_i)$;*
2. *$G$ is locally Lipschitz–continuous on $D$;*
3. *the derivatives of $G$ can be extended continuously to the boundary $\partial D_i$ such that*

$$\sup_{\mathbf{v} \in \overline{D}_i} \frac{\partial^k G}{\partial^{k_1} v_1 \cdots \partial^{k_{\overline{p}}} v_{\overline{p}}}(\mathbf{v}) \leq C_k$$

*for $k = \sum_{i=1}^{\overline{p}} k_i$, $k \in \{0, \dots, R\}$.*

This assumption has to hold for the numerical flux function $F : \mathbb{R}^{2p} \longmapsto \mathbb{R}$ as well as the numerical source function $S : \mathbb{R} \longmapsto \mathbb{R}$.

LEMMA 5.5. *(Finite differences for composite functions) Let the assumptions of Lemma 5.3 hold and assume that the nonlinear function $G$ satisfies Assumption 1. Introducing*

$$D_N(\mathbf{v}_L, K, \Sigma) := \sup\left\{|\Delta_K^N \mathbf{v}_{L,k'}| \ ; \ S(N,K,k') \subset \Sigma\right\} \quad \text{and}$$

$$I(R) := \left\{(\mathbf{j}, \mathbf{k}) \ ; \ \mathbf{j} \in \{1, \dots, R\}^R, \ \mathbf{k} \in \{0, \dots, R\}^R, \ \sum\nolimits_{r=1}^{R} j_r \, k_r = R\right\}, \tag{5.13}$$

*we obtain*

$$D_R(\mathbf{G}_L^n, K, \tilde{\Sigma}_{l,k,1}) \leq C \sup\left\{\prod\nolimits_{r=1}^{R} (D_{j_r}(\check{\mathbf{v}}_L^n, K, \tilde{\Sigma}_{l,k,1}^-))^{k_r} \ ; \ (\mathbf{j}, \mathbf{k}) \in I(R)\right\}. \tag{5.14}$$

The proof can be found in [9] or [18], Proposition 5, p. 104 in case of the numerical flux balances. It can also be applied to the numerical source function.

In order to further estimate the finite differences on the right hand side in (5.12) and (5.14) we need a discrete inverse estimate, i.e., we have to estimate the finite differences by details.

LEMMA 5.6. *(Discrete inverse estimate) Let $K \in \mathbb{N}$ be an arbitrary step size. Assume that the subdivision scheme converges uniformly in the sup–norm and the*

*corresponding primal wavelets $\psi_{j,k}$ are in $C^r$. For $N > 0$ we obtain*

$$|\Delta_K^N \check{v}_{L,k'}^n| \le C \sum_{l=-1}^{L-1} \min\{2^{-L+l+1}K, 1\}^{\min\{N,r\}} \sup\{|\check{d}_{l,k}^n| \; ; \; \Sigma_{l,k} \cap S(N,K,k') \neq \emptyset\}, \tag{5.15}$$

*where $\check{d}_{-1,k}^n := \check{v}_{0,k}^n$, $\Sigma_{-1,k} := \Sigma_{0,k,0}$ and $\Sigma_{l,k} := \Sigma_{l,k,1}$ for $l = 0, \dots, L-1$.*
The convergence of the subdivision scheme ensures the existence of the primal functions, see Theorem 2.1, and the uniform boundedness of the approximation error (2.11). Due to the dyadic grid refinement the limit functions are refinable functions for which an inverse estimate exists, cf. [7]. This is used to prove the assertion. For details, we refer to [9] or [18], Prop. 4, p. 101.

Then the details on the right hand side in (5.15) have to be estimated by the threshold values. Here the definition of the prediction set (5.8) enters. For this purpose, we now have to specify the the parameter $\sigma$ in the nesting (5.7) of the details.

Assumption 2. *Assume that the primal wavelets have $C^r$ Hölder smoothness, i.e., $\psi_{j,k} \in C^r$, and the dual wavelets have $M$ vanishing moments. Then we choose some $\sigma$ such that*

$$1 < \sigma < r + 1 \tag{5.16}$$

and fix the parameters $R$ and $\beta > 0$ such that

$$R - 1 < r \le R, \tag{5.17}$$

$$1 + \beta < \sigma < 1 + R - \beta. \tag{5.18}$$

The smoothness parameter $r$ is bounded by the number of vanishing moments $M$ of the dual wavelets $\tilde{\psi}_{j,k}$, i.e., $r < M$, and thus $\sigma < M + 1$ and $R \le M$.

Lemma 5.7. *(Stability of finite differences) Let the assumptions of Lemma 5.3 and 5.6 as well as Assumption 2 hold. Let $(l', k', e') \notin \tilde{\mathcal{D}}^{n+1}$, $N > 0$, $K \le C_K 2^{L-l'-1}$, where $C_K \in [1, \infty)$ is some constant independent of the levels $l'$ and $L$ and $k$ such that $S(N,K,k) \subset \tilde{\Sigma}^-_{l',k',e'}$. Then we get the estimate*

$$|\Delta_K^N \check{v}_{L,k}^n| \le C\, \varepsilon_{l'}^{\min\{N/R,1\}}, \tag{5.19}$$

*where the threshold values are given by $\varepsilon_l = 2^{l-L}\,\varepsilon$. In particular, if $N < R$ then the constant $C$ depends on $T$ and $u_0$.*
For a proof see [9] or [18], Prop. 7, p. 101.

Finally we obtain the reliability result for the original MR-FVS applied to the data of the modified MR-FVS, i.e., $\overline{\mathbf{v}}_L^{n+1} := \bar{\mathcal{E}}_{L,\bar{\mathcal{D}}^{n+1}} \mathcal{A}_{\bar{\mathcal{D}}^{n+1}} \check{\mathbf{v}}_L^n = \mathcal{A}_{\bar{\mathcal{D}}^{n+1}} \mathcal{E}_L \check{\mathbf{v}}_L^n$.

Theorem 5.8. *(Reliability) Let the Assumptions 1, 2 as well as the assumptions (A6) — (A11) of Lemma 5.3 hold true. Then the prediction set defined by (5.8) fulfills the reliability property (3.7).*

*Sketch of proof.* For some $(l', k', 1) \notin \tilde{\mathcal{D}}^{n+1}$ we have to verify that the detail $\overline{d}_{l',k'}^{n+1}$ can be estimated up to some constant by the threshold value $\varepsilon_{l'}$. For this purpose, we first estimate the detail on time level $n$ by finite differences according to Lemma 5.4. Then we apply the finite difference operator $\Delta_K^M$ to the evolution equations (3.1) with the numerical fluxes (3.4) and numerical sources (3.5) for level $l = L$. Finally we have to estimate the finite differences $\Delta_K^M \check{v}_{L,r}^n$ and $\Delta_K^M B_{L,r}^n$, $\Delta_K^M S_{L,r}^n$ by Lemma

5.7 and 5.5, respectively. Details on the proof can be found in [9] or [18], Theorem 7, p. 110. ∎

For the prediction strategy developed in [9] this could be verified under the same assumptions. There it was proven only for *homogeneous* conservation laws. However, the proof will also work in case of inhomogeneous equations where we have to replace in the proof $B_{L,k}$ by $B_{L,k} - \tau\, S_{L,k}$ with *exact* source reconstruction.

**5.3. Error of approximate reconstruction.** It remains to verify assumption (A2) in Theorem 5.1. For this purpose, we first derive sufficient conditions which are verified to hold for the approximate flux and source reconstruction (4.5), (4.6), (4.7) and (4.11), (4.12), (4.13), respectively.

THEOREM 5.9. *(Sufficient condition) The above assumptions hold true. Assume that in particular for the CFL-condition we have*

$$\frac{\tau}{h_L} \max_{|u|\le C(T,u_0)} |f'(u)| \le C < 1 \tag{5.20}$$

*with $C(T,u_0)$ given by (5.9) in Lemma 5.3. Then the approximate flux and source reconstruction is accuracy preserving, i.e., (A2) holds true, provided that*

$$|\bar F^n_{l,k} - \check F^n_{l,k}| \lesssim \varepsilon, \quad \forall (l,k) \in \mathcal{F}(\tilde{\mathcal{D}}^{n+1}), \tag{5.21}$$

*and*

$$|\bar S^n_{l,k} - \check S^n_{l,k}| \lesssim 2^l \varepsilon, \quad \forall (l,k) \in \mathcal{S}(\tilde{\mathcal{D}}^{n+1}). \tag{5.22}$$

*Proof.* Let be $\bar{\mathbf{w}}^{n+1}_L := \bar{\mathcal{E}}_{L,\bar{\mathcal{D}}^{n+1}} \check{\mathbf{w}}^n_L$, $\check{\mathbf{w}}^{n+1}_L := \check{\mathcal{E}}_{L,\bar{\mathcal{D}}^{n+1}} \check{\mathbf{w}}^n_L$. Then we may represent the error of the subdivision scheme (3.9) as

$$\bar{\mathbf{w}}^{n+1}_L - \check{\mathbf{w}}^{n+1}_L = \sum_{(l,k,e)\in\bar{\mathcal{D}}^{n+1}} \mathbf{\Psi}^L_{l,r,e} (\bar d^{n+1}_{l,r,e} - \check d^{n+1}_{l,r,e}),$$

which can be estimated by

$$\|\bar{\mathbf{w}}^{n+1}_L - \check{\mathbf{w}}^{n+1}_L\| \le \sum_{(l,r,e)\in\bar{\mathcal{D}}^{n+1}} \|\mathbf{\Psi}^L_{l,r,e}\|\, |\bar d^{n+1}_{l,r,e} - \check d^{n+1}_{l,r,e}|.$$

The norm of the discrete basis vectors can be represented as

$$\|\mathbf{\Psi}^L_{l,k,e}\| = \sum_{r\in\Sigma^L_{l,k,e}} |V_{L,r}|\, |(\mathbf{\Psi}^L_{l,k,e})_r|$$

where $\Sigma^L_{l,k,e} \subset I_L$ is the support of $\mathbf{\Psi}^L_{l,k,e}$. Next we conclude from Theorem 2.1

$$|(\mathbf{\Psi}^L_{l,k,e})_r| = |\langle \psi_{l,k,e}, \tilde\phi_{L,r}\rangle| \le \|\psi_{l,k,e}\|_{L^\infty} \lesssim 1$$

and

$$\left|\bigcup\nolimits_{r\in\Sigma^L_{l,k,e}} V_{L,r}\right| = |\operatorname{supp}\, \psi_{l,k,e}| \lesssim 2^{-l}.$$

Hence the error can be further estimated by

$$\|\bar{\mathbf{w}}^{n+1}_L - \check{\mathbf{w}}^{n+1}_L\| \lesssim \sum_{(l,r,e)\in\bar{\mathcal{D}}^{n+1}} 2^{-l} |\bar d^{n+1}_{l,r,e} - \check d^{n+1}_{l,r,e}|.$$

From the evolution equations (3.2) and (3.3) together with exact and approximate flux and source reconstruction as well as the identity (2.7), we obtain for the difference of the details

$$|\bar{d}^{n+1}_{l,r,e} - \check{d}^{n+1}_{l,r,e}| = \left| \sum_{s\in\mathcal{M}^e_{l,r}} m^{l,e}_{s,r}\lambda_{l+1,s}(\bar{B}^n_{l+1,s} - \check{B}^n_{l+1,s}) + \tau \sum_{s\in\mathcal{M}^e_{l,r}} \left(\bar{S}^n_{l+1,s} - \check{S}^n_{l+1,s}\right) \right| \lesssim$$
$$\max_{s\in\mathcal{M}^e_{l,r}} \lambda_{l+1,s} \left|\bar{B}^n_{l+1,s} - \check{B}^n_{l+1,s}\right| + \tau \max_{s\in\mathcal{M}^e_{l,r}} \left|\bar{S}^n_{l+1,s} - \check{S}^n_{l+1,s}\right| \tag{5.23}$$

because the supports $\mathcal{M}^e_{l,r}$ and the mask coefficients $m^{l,e}_{s,r}$ are uniformly bounded, see (2.3) and (2.6).

From the definition of the flux balances as well as the sources we infer from assumption (5.21) and (5.22)

$$\|\bar{\mathbf{w}}^{n+1}_L - \check{\mathbf{w}}^{n+1}_L\| \lesssim \sum_{(l,r,e)\in\tilde{\mathcal{D}}^{n+1}} \frac{\tau}{h_{l+1}} 2^{-l}\,\varepsilon + \sum_{(l,r,e)\in\tilde{\mathcal{D}}^{n+1}} \tau\varepsilon.$$

The number of significant details is bounded by that of all possible coefficients

$$\#\tilde{\mathcal{D}}^{n+1} \le \#I_0 + \sum_{l=0}^{L-1} \#I_l = N_0 + N_0 \sum_{l=0}^{L-1} 2^l = N_0\, 2^L.$$

Since $h_l = 2^{L-l}h_L$ and $h_L = 2^{-L}h_0$, respectively, and the CFL-condition (5.20) holds we finally obtain

$$\|\bar{\mathbf{w}}^{n+1}_L - \check{\mathbf{w}}^{n+1}_L\| \lesssim \sum_{(l,r,e)\in\tilde{\mathcal{D}}^{n+1}} \frac{\tau}{h_L} 2^{l+1-L}\, 2^{-l}\,\varepsilon + \sum_{(l,r,e)\in\tilde{\mathcal{D}}^{n+1}} \tau\varepsilon$$
$$\lesssim N_0\, 2^L \left(2\cdot\, 2^{-L} + h_0\, 2^{-L} \max_{|u|\le C(T,u_0)} |f'(u)|\right) \varepsilon \lesssim \varepsilon.$$

□

**5.3.1. Approximate flux reconstruction.** In order to verify the sufficient condition (5.21) for the approximate flux reconstruction we proceed in several steps. First of all, we have to estimate the error introduced by polynomial reconstruction.

LEMMA 5.10. *(Error of polynomial reconstruction) Let $x_k = kh$, $h > 0$, $k \in \mathbb{Z}$, be a uniform discretization of the real line and $v_k$ be data to the cell $[x_k, x_{k+1}]$. Let $k$ be fixed, $R^N_k \in \Pi_N$ denotes the reconstruction polynomial to the stencil $\mathcal{S}_k := \{\underline{k}, \dots, \overline{k}\}$ for some $\underline{k} \in \{k-N, \dots, k\}$ and $\overline{k} = \underline{k} + N$ with*

$$\hat{P}_{k'} := \frac{1}{h}\int_{x_{k'}}^{x_{k'+1}} R^N_k(x)\,dx = v_{k'} \quad \forall k' \in \mathcal{S}_k. \tag{5.24}$$

*Then the error between the reconstructed cell average $\hat{P}_{k'}$ and the cell average $v_{k'}$ is either zero, i.e., $v_{k'} = \hat{P}_{k'}$, $k' \in \mathcal{S}_k$, or can be represented as a linear combination of finite differences of order $N+1$, i.e.,*

$$v_{k'} - \hat{P}_{k'} = \begin{cases} \sum_{j=0}^{\underline{k}-k'-1} \alpha_{k',j}\Delta_1^{N+1} v_{k'+j}, & k' < \underline{k}, \\ \sum_{j=0}^{k'-\overline{k}-1} \alpha_{k',j}\Delta_1^{N+1} v_{k'-N-j-1}, & \overline{k} < k', \end{cases}$$

*where the coefficients $\alpha_{k',j}$ only depend on $N$.*

*Sketch of proof.* For $k' \in \mathcal{S}_k$ the reconstruction condition (4.1) holds, i.e., the error vanishes. For $k' \notin \mathcal{S}_k$ the proof follows by induction starting at $k' = \underline{k} - 1$ and $k' = \overline{k} + 1$, respectively. Here we make use of the representation (4.4) of the reconstruction polynomial via the interpolation polynomial (4.3) of the primitive function. In particular, we employ that $(N+1)$-st order finite differences of the interpolation polynomial $Q_k^{N+1}$ are constant and, hence, $\Delta_1^{N+1} \hat{P}_r = 0$. The complete proof is given in Appendix 7.2. ∎

Next we rewrite finite differences on level $l$ by those on higher levels with larger step size.

LEMMA 5.11. *For finite differences of order $N \in \mathbb{N}$ the two-scale relation*

$$\Delta_1^N v_{l,k} = \frac{1}{2} \sum_{i=0}^{N+1} \binom{N+1}{i} \Delta_1^N v_{l+1,2k+i} \tag{5.25}$$

*holds. Alternatively, finite differences can be represented by a sum of finite differences on level $L$ with step size $2^{L-l}$, i.e.,*

$$\Delta_1^N v_{l,k} = 2^{l-L} \sum_{\nu=0}^{2^{L-l}-1} \Delta_{2^{L-l}}^N v_{L,2^{L-l}k+\nu}. \tag{5.26}$$

*Sketch of proof.* The proof is elementary. Relation (5.25) follows by induction using the addition theorem for binomial coefficients whereas (5.26) is a straight-forward calculation employing the encoding (2.3) and the definition (5.10) of the finite difference. Details can be found in the Appendix 7.3. ∎

Similar to Lemma 5.7 we can now estimate the finite differences on level $l$ instead of level $L$.

LEMMA 5.12. *Assume that the dual wavelets have $M = 2s+1 \geq N+1$ vanishing moments. Given a sequence of averages $\mathbf{v}_L$ with multiscale decomposition $\{d_{j,k,e}\}_{(j,k,e)\in\mathcal{D}}$. Let $\mathcal{G} = \mathcal{G}(\mathcal{D})$ be the adaptive grid corresponding to the set of significant details $\mathcal{D}$ that is graded of degree $q \geq \lceil \frac{3s}{2} \rceil$. Then for any $(l,k) \in \mathcal{G}$ we have*

$$|\Delta_1^{N+1} v_{l,k'}| \lesssim \varepsilon_l^{\min\left(\frac{N+1}{R},1\right)}, \quad \forall k' \in \{k-2s, \dots, k+2s-N-1\}$$

*provided that the assumptions of Lemma 5.7 hold true.*

*Sketch of proof.* The basic idea is to rewrite the finite difference $\Delta_1^{N+1} v_{l,k'}$ on level $l$ in a series of finite differences $\Delta_{2^{L-l-1}}^{N+1} v_{L,2^{L-l-1}(2k'+i)+\mu}$, $i = 0, \dots, N+2$, $\mu = 0, \dots, 2^{L-l-1}-1$ on level $L$ first applying (5.25) and then (5.26). For each of these differences we have to verify that its stencil is included in a backward influence set $\tilde{\Sigma}^-_{l+1,2k+q',1}$ defined by (5.6) for some $q'$ such that $(l+1, 2k+q') \notin \mathcal{D}$. It turns out that $q' \in \{-3s, \dots, 3s+1\}$. On the other hand we deduce from the grading procedure and the assumption $(l,k) \in \mathcal{G}$, i.e., $(l,k) \notin \mathcal{D}$, that the range of dependence for $(l,k)$ on level $l+1$ is determined by $\tilde{\Sigma}_{l,k}^{\mathcal{G},(l+1)} = \{2(k-q), \dots, 2(k+q)+1\}$. Then choosing the grading parameter sufficiently large ensures that $2k+q' \in \tilde{\Sigma}_{l,k}^{\mathcal{G},(l+1)}$. Finally, we may apply Lemma 5.7 and the assertion follows. For a detailed proof see Appendix 7.4. ∎

Note that in Lemma 5.12 the order $N$ of the finite difference is not yet limited to the degree of the reconstruction polynomial. In particular, it might be the starting

point to construct an *hp*-version of the adaptive multiscale scheme. The idea would be to look for the smallest $N$ such that

$$|\Delta_1^{N+1} v_{l,k'}| \lesssim \varepsilon_l$$

holds. This would imply

$$|\langle R_{l,k}^N, \tilde{\varphi}_{L,r}\rangle - v_{L,r}| \lesssim \varepsilon_l, \quad \forall r \in \{2^{L-l}k, \dots, 2^{L-l}(k+1)-1\}$$

in Lemma 5.13 and in the proof of Theorem 5.14 below.

Next we estimate the error between the averages and the reconstructed averages.

LEMMA 5.13. *Assume that the dual wavelets have $M = 2s+1 \geq N+1$ vanishing moments, where $N$ is the degree of the reconstruction polynomial. Given a sequence of averages $\mathbf{v}_L$ with multiscale decomposition $\{d_{j,k,e}\}_{(j,k,e)\in\mathcal{D}}$. Let $\mathcal{G} = \mathcal{G}(\mathcal{D})$ be the adaptive grid corresponding to the set of significant details $\mathcal{D}$ that is graded of degree $q \geq \lceil \frac{3s}{2} \rceil$. Then for any $(l,k) \in \mathcal{G}$ we have*

$$|\langle R_{l,k}^N, \tilde{\varphi}_{L,r}\rangle - v_{L,r}| \lesssim \max\left(\varepsilon_l^{\min\left(\frac{N+1}{R},1\right)}, \varepsilon_l\right), \quad r \in \{2^{L-l}k, \dots, 2^{L-l}(k+1)-1\}$$

*provided that (i) the subdivision scheme converges uniformly in the* sup*-norm, (ii) the reconstruction stencil $\mathcal{S}_{L,k}$ is lying inside the support $\bigcup_{r=2^{L-l}k}^{2^{L-l}(k+1)-1} \bar{\Sigma}_{L,r,0}^{(l)}$ of the subdivision scheme and (iii) the assumptions of Lemma 5.7 hold true.*

*Sketch of proof.* The basic idea is to apply the subdivision scheme (2.8) to the reconstructed averages $\hat{P}_{L,r} := \langle R_{l,k}^N, \tilde{\varphi}_{L,r}\rangle$ and the cell averages $v_{L,r}$, respectively, and to estimate the difference of both series: (i) Since the number of vanishing moments $M$ is larger than the degree $N$ of the reconstruction polynomial, the details corresponding to the multiscale decomposition of the reconstruction polynomial vanish. (ii) Assuming that the grading parameter satisfies $q \geq s$ we conclude that the support of the wavelets $\bar{\Sigma}_{L,r,1}^{(j)}$ is included in the range of dependence $\tilde{\Sigma}_{l,k}^{\mathcal{G},(j)}$ for all $r \in \{2^{L-l}k, \dots, 2^{L-l}(k+1)-1\}$ and $j = l+1, \dots, L-1$. Hence , the details $d_{j,k'}$, $k' \in \tilde{\Sigma}_{l,k}^{\mathcal{G},(j)}$, corresponding to the cell averages are not significant. On the other hand, the remaining details $d_{l,k'}$, $k' \in \bar{\Sigma}_{L,r,1}^{(l)} \subset \{k-s, \dots, k+s\}$ can be estimated by $|d_{l,k'}| \leq 2^\sigma \varepsilon_l$ due to the definition of the prediction set (5.8) where $\sigma$ is a constant which is fixed in Assumption 2. (iii) The differences between the cell averages $v_{l,k'}$ and $P_{l,k'}$ for $k' \in \bar{\Sigma}_{L,r,0}^{(l)}$ can be estimated by Lemma 5.10 and 5.12. The details of the proof are given in Appendix 7.5. ∎

Finally we can verify the sufficient condition (5.21) in case of approximate flux reconstruction.

THEOREM 5.14. *Assume that the primal wavelets have Hölder regularity $C^r$, $0 < r \leq N+1$, and the parameters $R$ and $\beta$ are chosen according to Assumption 2. Furthermore the adaptive grid is assumed to be graded of degree $q \geq \lceil \frac{3s}{2} \rceil$ and the dual wavelets have $M = 2s+1 \geq N+1 \geq R$ vanishing moments where $N$ is the degree of the polynomial reconstruction and $R$ is the parameter chosen in Assumption 2. Then the error between exact and approximate flux reconstruction strategy determined by (3.4) and (4.5), (4.6), (4.7), respectively, can be estimated by*

$$|\bar{F}_{l,k}^n - \check{F}_{l,k}^n| \lesssim \varepsilon, \qquad (l,k) \in \mathcal{F}_{\bar{\mathcal{D}}^{n+1}}. \tag{5.27}$$

*Proof.* Let $(l,k) \in \mathcal{F}_{\tilde{\mathcal{G}}^{n+1}}$, $l \in \{0,\dots,L-1\}$. Since $F$ is assumed to be locally Lipschitz-continuous with constant $L_F$, see Assumption 1, we can estimate the error between the exact and approximate flux reconstruction (3.4) and (4.5), respectively, by

$$|\bar{F}_{l,k} - \check{F}_{l,k}| = |F(v_{L,2^{L-l}k-p},\dots,v_{L,2^{L-l}k+p-1}) - F(w_{l,2^{L-l}k-p},\dots,w_{l,2^{L-l}k+p-1})| \leq L_F \sum_{i=-p}^{p-1} |v_{L,2^{L-l}k+i} - w_{l,2^{L-l}k+i}|. \tag{5.28}$$

For simplicity of representation we suppress the time index.

Here the values $w_{L,k'}$, $k' \in \{2^{L-l}k-p,\dots,2^{L-l}k+p-1\}$ are determined by polynomial reconstruction according to (4.1) and (4.2), i.e.,

$$w_{L,k'} = \frac{1}{|V_{L,k'}|} \int_{V_{L,k'}} R^N_{l',r'}(x)\,dx.$$

Note that in the neighborhood of a cell $V_{l,k}$ the neighboring cells in the adaptive grid $\mathcal{G}$ are not necessarily sitting on the same level. Therefore the average $w_{L,k'}$ is computed by the reconstruction polynomial $R^N_{l',r'}$ on level $l' = l'(k')$ related to the cell $V_{l',r'} \subset V_{L,k'}$ with $r' = r'(k')$ where $(l',r') \in \tilde{\mathcal{G}}^{n+1}$, see Fig. 5.2.

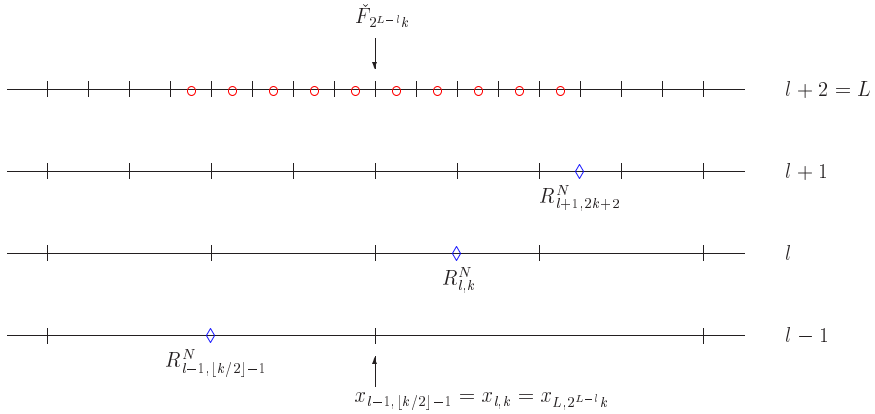


FIG. 5.2. *Illustration of approximate flux reconstruction at the interface $x_{l,k}$ in case of $p=5$. The locally adapted grid is indicated by the cell midpoints ◊. For the flux computation the data on level $L$ indicated by ○ have to be computed by the reconstruction polynomials $R^N_{l-1,\lfloor k/2\rfloor-1}$, $R^N_{l,k}$ and $R^N_{l+1,2k+2}$, respectively.*

Since the grid is assumed to be graded, the number of different levels is uniformly bounded, i.e.,

$$|l'-l| \leq C$$

with $C$ only depending on $s$ and $p$. Hence, we can estimate the difference on the right-hand side in (5.28) by Lemma 5.13

$$|v_{L,k'} - w_{L,k'}| = |v_{L,k'} - \langle R^N_{l',k'}, \tilde{\varphi}_{L,k'}\rangle| \lesssim \varepsilon_{l'}^{\min\{\frac{N+1}{R},1\}} \lesssim \varepsilon_l^{\min\{\frac{N+1}{R},1\}} = \varepsilon_l, \tag{5.29}$$

because $(N+1)/R \geq 1$ due to assumption. Then the assertion follows by the choice of $\varepsilon_l = 2^{l-L}\varepsilon$.

In the second case (4.6) where $(l,k) \notin \mathcal{F}_{\tilde{\mathcal{G}}^{n+1}}$ and there exists $j \in \{l+1,\dots,L\}$ such that $(l',k') := (j, 2^{j-l}k) \in \mathcal{F}_{\tilde{\mathcal{G}}^{n+1}}$ the numerical fluxes are determined by

$$\bar{F}_{l,k} = \bar{F}_{j,2^{j-l}k} = \bar{F}_{L,2^{L-l'}k'} = F(v_{L,2^{L-l'}k'-p},\dots,v_{L,2^{L-l'}k'+p-1}),$$
$$\check{F}_{l,k} = \check{F}_{j,2^{j-l}k} = \check{F}_{l',k'} = F(v_{l',k'-p},\dots,v_{l',k'+p-1}).$$

Then (5.29) also holds true with $\varepsilon_{l'}$ instead of $\varepsilon_l$ where we apply the above analysis to $(l',k')$ instead of $(l,k)$.

In the last case (4.7), where there is no $j \in \{0,\dots,L\}$, such that $(j,2^{j-l}) \in \mathcal{F}_{\tilde{\mathcal{G}}^{n+1}}$, but there is $j' = \max\{j \,|\, (j,2^{j-l}k) \in \mathcal{F}_{\tilde{\mathcal{D}}^{n+1}}\}$, we apply the above analysis to $(l',k') := (j', 2^{j'-l})$. ∎

**5.3.2. Approximate source reconstruction.** For verification of the sufficient condition (5.22) for the approximate source reconstruction we can not directly apply Lemma 5.13 because of the composition of the source function and the sliding average of the reconstruction polynomial. Here we have first to estimate the differences of the composite function similar to Lemma 5.5

LEMMA 5.15. *(Boundedness of derivatives of composite function) Let the assumptions of Lemma 5.3 hold true. Furthermore the source function $S$ satisfies Assumption 1. Let $\mathcal{V}$ be the sliding average of the reconstruction polynomial $R_{l,k}^N$ to cell $V_{l,k}$ and $(l,k) \in \mathcal{G}(\mathcal{D})$. Then the $R$-th derivative of the composite function $G = S \circ \mathcal{V}$ is bounded by*

$$\sup_{x \in V_{l,k}} |G^{(R)}(x)| \lesssim h_l^{2-R}\varepsilon_l$$

*for $0 \leq R \leq N$.*

*Sketch of proof.* The proof is similar to the one for Lemma 5.5 that can be found in [9] or [18], Proposition 5, p. 104. The basic idea is to estimate the $R$-th derivative of the composite function $G$ by means of finite differences $\Delta_1^j v_{l,k'}$ of order $j = 0,\dots,R$. For this purpose, we have to estimate the $j$-th derivative of the sliding average $\mathcal{V}$. According to (4.10) the latter is defined by the interpolation polynomial $Q_{l,k}^{N+1}$ that is determined by the interpolation conditions (4.3). Hence, we have to estimate the $j$-th derivative of $Q_{l,k}^{N+1}$. Here it is most convenient to consider the Newton representation because therein the finite differences naturally occur. Finally, the finite differences can be estimated by Lemma 5.12. Details of the proof are given in Appendix 7.6. ∎

Finally we can verify the sufficient condition (5.22) in case of approximate source reconstruction.

THEOREM 5.16. *Assume that the primal wavelets have Hölder regularity $C^r$, $0 < r \leq N+1$, and the parameters $R$ and $\beta$ are chosen according to Assumption 2. Furthermore the adaptive grid is assumed to be graded of degree $q \geq \lceil \frac{3s}{2} \rceil$ and the dual wavelets have $M = 2s+1 \geq N+1 \geq R$ vanishing moments where $N$ is the degree of the polynomial reconstruction and $R$ is the parameter chosen in Assumption 2. Then the error between the exact and approximate source reconstruction strategy determined by (3.5) and (4.11), (4.12), (4.13), respectively, can be estimated by*

$$|\bar{S}_{l,k}^n - \check{S}_{l,k}^n| \lesssim \varepsilon, \qquad (l,k) \in \mathcal{S}_{\tilde{\mathcal{D}}^{n+1}}. \tag{5.30}$$

*Proof.* First of all we consider $(l,k) \in \tilde{\mathcal{G}}^{n+1} \subset \mathcal{S}_{\tilde{\mathcal{D}}^{n+1}}$. Due to (3.5) the exact source reconstruction in cell $V_{l,k}$ is given by

$$\bar{S}_{l,k} = 2^{l-L} \sum_{i=0}^{2^{L-l}-1} \bar{S}_{L,2^{L-l}k+i} = 2^{l-L} \sum_{i=0}^{2^{L-l}-1} S(v_{L,2^{L-l}k+i}).$$

We now introduce the approximation

$$\tilde{S}_{l,k} := 2^{l-L} \sum_{i=0}^{2^{L-l}-1} S(\mathcal{V}(\hat{x}_{L,2^{L-l}k+i})) = \frac{1}{h_l} \sum_{i=0}^{2^{L-l}-1} h_L S(\hat{P}_{L,2^{L-l}k+i}),$$

where $\mathcal{V}$ is the sliding average determined by the polynomial reconstruction $R_{l,k}^N$ to cell $V_{l,k}$, $\hat{P}_{L,2^{L-l}k+i}$ is the cell average of $R_{l,k}^N$ in cell $V_{L,2^{L-l}k+i}$ and $\hat{x}_{L,2^{L-l}k+i} = x_{L,2^{L-l}k+i} + \frac{h_L}{2}$ is the midpoint of cell $V_{L,2^{L-l}k+i}$. Note that $\mathcal{V}(\hat{x}_{L,2^{L-l}k+i}) = \hat{P}_{L,2^{L-l}k+i}$ because of the construction of the reconstruction polynomial (4.3), (4.4) and the definition of the sliding average (4.10). Obviously, $\tilde{S}_{l,k}$ is the midpoint quadrature rule applied to the subintervals $V_{L,2^{L-l}k+i}$, $i = 0, \dots, 2^{L-l}-1$, approximating the integral

$$I_{l,k} := \frac{1}{h_l} \int_{V_{l,k}} G(x)\, dx = \frac{1}{h_l} \sum_{i=0}^{2^{L-l}-1} \int_{V_{L,2^{L-l}k+i}} G(x)\, dx \tag{5.31}$$

with the composite function $G = S \circ \mathcal{V}$.

Note that $h_L = 2^{l-L} h_l$. The error can be estimated by

$$|I_{l,k} - \tilde{S}_{l,k}| \le \frac{1}{24} h_L^2 \sup_{x \in V_{l,k}} |G^{(2)}(x)|. \tag{5.32}$$

On the other hand, the approximate reconstruction of the source in cell $V_{l,k}$ according to the strategy is given by some quadrature rule applied to the integral (5.31), i.e.,

$$\check{S}_{l,k} = \frac{1}{h_l} \sum_{i=0}^{m} w_i S(\mathcal{V}(x_i)) = \frac{1}{h_l} \sum_{i=0}^{m} w_i G(x_i)$$

for some nodes $x_i \in V_{l,k}$ and some weights $w_i$, $i = 0, \dots, m$.

Assume that the error can be estimated by

$$|I_{l,k} - \check{S}_{l,k}| \lesssim h_l^{\alpha} \sup_{x \in V_{l,k}} |G^{(\alpha)}(x)| \tag{5.33}$$

for some integer $\alpha = \alpha(m)$.

The error between exact and approximate source reconstruction can now be split into two parts

$$|\bar{S}_{l,k} - \check{S}_{l,k}| \le |\bar{S}_{l,k} - \tilde{S}_{l,k}| + |\tilde{S}_{l,k} - \check{S}_{l,k}|. \tag{5.34}$$

The first term can now be estimated

$$|\bar{S}_{l,k} - \tilde{S}_{l,k}| \le L_s \max_{i=0,\dots,2^{L-l}-1} |v_{L,2^{L-l}k+i} - \hat{P}_{L,2^{L-l}k+i}| \lesssim \max\left(\varepsilon_l^{\min\left(\frac{(N+1)}{R},1\right)}, \varepsilon_l\right) \tag{5.35}$$

due to the local Lipschitz continuity of $S$ and Lemma 5.13.

The second term in (5.34) is again split into two parts accounting for the integration error, i.e.,

$$|\tilde{S}_{l,k} - \check{S}_{l,k}| \leq |\tilde{S}_{l,k} - I_{l,k}| + |I_{l,k} - \check{S}_{l,k}|.$$

From Lemma 5.15 the errors (5.32) and (5.33) are bounded up to some constant

$$|\tilde{S}_{l,k} - \check{S}_{l,k}| \lesssim h_L^2 \varepsilon_l + h_l^\alpha h_l^{2-\alpha} \varepsilon_l \lesssim \varepsilon_l. \tag{5.36}$$

Since $(N+1)/R \geq 1$ the assertion follows from (5.34), (5.35) and (5.36) by the choice of $\varepsilon_l = 2^{l-L}\varepsilon$.

In the second case when $(l,k) \notin \tilde{\mathcal{G}}^{n+1}$ but there exists $j \in \{l+1, \ldots, L\}$ such that $(j, 2^{j-l}k) \in \tilde{\mathcal{G}}^{n+1}$ we infer from (3.5) and (4.12)

$$|\bar{S}^n_{l,k} - \check{S}^n_{l,k}| \leq \sum_{i=0}^{2^{j-l}-1} 2^{l-j} |\bar{S}^n_{j,2^{j-l}k+i} - \check{S}^n_{j,2^{j-l}k+i}| \leq \max_{i=0,\ldots,2^{j-l}-1} |\bar{S}^n_{j,2^{j-l}k+i} - \check{S}^n_{j,2^{j-l}k+i}|.$$

Then (5.30) holds true with $\varepsilon_j$ instead of $\varepsilon_l$.

In the last case where there $j \in \{0, \ldots, l-1\}$ exists such that $(l', k') := (j, \lfloor k/2^{l-j} \rfloor) \in \tilde{\mathcal{G}}^{n+1}$ we infer from (4.13)

$$\bar{S}^n_{l,k} - \check{S}^n_{l,k} = \bar{S}^n_{l,k} - \check{S}^n_{l',k'} + \bar{S}^n_{l',k'} - \bar{S}^n_{l,k} = \bar{S}^n_{l',k'} - \check{S}^n_{l',k'}.$$

We now apply again the above analysis to $(l', k')$. ∎

Note that the estimate (5.30) can be proven for any $\alpha$ in the quadrature error (4.9) and (5.33), respectively. Therefore, we may use the midpoint rule, i.e. $m = 0$. Hence only *one* function evaluation is required in case of (4.11).

**6. Numerical results.** The analytical results are now to be verified by numerical computations. For this purpose we consider the inhomogeneous, inviscid Burgers equation, i.e., $f(u) = 0.5u^2$ with source $s(u) = u\,(u - 0.5)\,(u - 1)$ and initial data $u_0(x) = \sin(2\,\pi\,x)$.

The computational domain $\Omega = [0, 1]$ is discretized by $N_0 = 10$ cells on the coarsest level, i.e., $h_0 = 0.1$. Hence the resolution for higher refinement levels is $N_l = 2^l\,N_0$ and $h_l = 2^{-l}\,h_0$. At the boundaries we use periodic boundary conditions. For the time discretization we have to respect the CFL condition. Here we choose $\tau_0 = 0.016$ and the final integration time is $T = 0.24$. Since we perform a global time stepping the CFL condition has to hold for the smallest cells corresponding to the highest refinement level $L$, i.e., $\tau = 2^{-L}\,\tau_0$. For the multiscale analysis we use wavelets with $M = 2\,s + 1 = 3$ vanishing moments, see Table 2.1, and the grading parameter is chosen as $q = 2s = 2$. Instead of using the prediction strategy according to Section 5.2.1 we apply Harten's original strategy although this has not yet been proven to be reliable but is always used in practice, cf. [4].

The reference FVS (1.3) is determined by the Godunov flux $F_k = F^G(v_k^L, v_k^R) = F(v_{k-2}, \ldots, v_{k+1})$. In order to improve spatial and temporal accuracy we employ a piecewise linear ENO reconstruction, cf. [15]. For a non-equidistant grid this reads

$$\begin{aligned} v_k^L &= v_{k-1} + \overline{m}\,(\Delta\,v_k, \Delta\,v_{k-1})\;(h_{k-1} - \tau\,f'(v_{k-1} + \overline{m}\,(\Delta\,v_k, \Delta\,v_{k-1})\;h_{k-1})) \\ v_k^R &= v_k - \overline{m}\,(\Delta\,v_{k+1}, \Delta\,v_k)\;(h_k + \tau\,f'(v_k - \overline{m}\,(\Delta\,v_{k+1}, \Delta\,v_k)\;h_k)) \end{aligned}$$

with the divided differences $\Delta v_i := (v_i - v_{i-1})/(h_i + h_{i-1})$ and the minmod function $\overline{m}$ defined by $\overline{m}(a,b) := a$ if $|a| \leq |b|$ and $\overline{m}(a,b) := b$ elsewhere. Note that the term corresponding to the time discretization $\tau$ guarantees second order in time. For the source term we apply the first order approximation (1.5).

Computations have been performed for varying threshold values $\varepsilon$ and different flux and source reconstruction strategies: (i) flux and source computation on unstructured meshes using only local data corresponding to the adaptive grid as is frequently used in applications, cf. [4], (ii) approximate reconstruction strategy according to (4.5), (4.6) and (4.11), (4.12) using the midpoint rule and reconstruction polynomials of degree $N = 2\,s = 2$ with central stencil $\mathcal{S}_{l,k} = \{k - s, \ldots, k + s\}$, and (iii) exact reconstruction strategy according to (3.4) and (3.5). These are referred to RM=1,2,3 in Figures 6.4, 6.5, 6.3 and 6.2.

The solution is developing a shock at time $t = 1/\pi$ in position $x = 0.5$ which is is moving at negative speed due to the inhomogeneity. In Figure 6.1 we present the adaptive solution for $L = 10$, $\varepsilon = 10^{-3}$ by points at the cell center of the adaptive grid and the *exact* solution computed by the reference scheme on a uniform grid corresponding to $L = 14$.

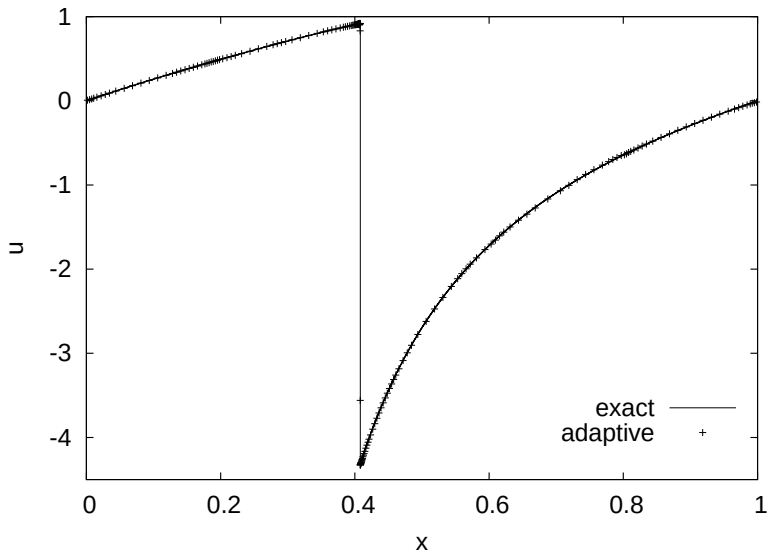


FIG. 6.1. *Comparison of adaptive solution ($L = 10$, $\varepsilon = 10^{-3}$) and* exact *solution ($L = 14$, $\varepsilon = 0$)*

To investigate the influence of the different flux and source reconstruction strategies on the efficiency of the adaptive scheme we have to consider the computational effort (memory and CPU) and the accuracy (discretization and perturbation error) for varying threshold values. All adaptive computations are performed with $L = 10$ refinement levels.

According to the ideal strategy in Section 5 the threshold value $\varepsilon$ has to be chosen such that the discretization error $\boldsymbol{\tau}_L = \hat{\mathbf{u}}_L - \mathbf{v}_L$ of the reference scheme and the perturbation error $\mathbf{e}_L = \mathbf{v}_L - \overline{\mathbf{v}}_L$ are balanced. For $L = 10$ we obtain $\|\boldsymbol{\tau}_L\| = 5.8 \times 10^{-4}$ where the "exact " solution is obtained by the FVS on a uniform mesh corresponding to $L = 14$ refinement levels.

First we consider the perturbation error due to thresholding plotted in Figure

6.2 for varying threshold parameters. Obviously, the perturbation error is decreasing with smaller threshold values. In particular, $\|\mathbf{e}_L\| \to 0$ for $\varepsilon \to 0^+$, i.e., the adaptive scheme is converging to the reference solution obtained on the reference grid with $L$ refinement levels. Of course, we do not gain in accuracy when choosing a too small threshold value because the discretization error is fixed by the number of refinement levels.

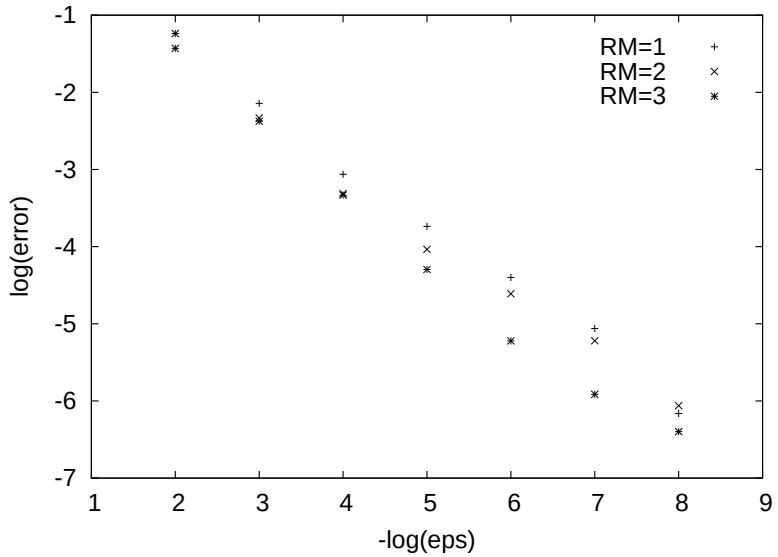


FIG. 6.2. *Perturbation error of adaptive solution ($L = 10$, varying threshold value $\varepsilon$) and reference solution ($L = 10$, $\varepsilon = 0$) on reference grid ($L = 10$)*

To determine the optimal threshold value we plot the error $\|\hat{\mathbf{u}}_L - \overline{\mathbf{v}}_L\|$ of the adaptive scheme (5.1) for different threshold values, see Figure 6.3. From this we conclude that an optimal choice would be $\varepsilon_{opt} \in [10^{-5}, 10^{-4}]$ because the error of the adaptive scheme is decreasing with decreasing threshold value $\varepsilon$ as long as $\varepsilon > \varepsilon_{opt}$ whereas it stalls for $\varepsilon < \varepsilon_{opt}$. Hence, for $\varepsilon > \varepsilon_{opt}$ the perturbation error due to thresholding is dominating whereas for $\varepsilon < \varepsilon_{opt}$ the discretization error is dominating.

The above observations concerning the discretization and perturbation error hold true independent of the flux and source reconstruction strategy. However, for a threshold value $\varepsilon_{opt}$ in the optimal range we depict from Figures 6.2 and 6.3 that the highest accuracy is obtained with the exact strategy (RM=3). For the approximate strategy (RM=2) we are loosing a bit in accuracy, but for the local strategy (RM=1) the loss is much more severe.

To conclude on the efficiency of the different strategies we have to consider the computational costs. First we discuss the size of the adaptive grids that determine the memory requirements, see Figure 6.4. We note that the minimal grid size is usually obtained for the exact strategy (RM=3) whereas for the local (RM=1) and the approximate (RM=2) strategy we need more cells. This might be caused by small oscillations induced by the reconstruction error. This becomes more severe in case of the local strategy (RM=1) if the threshold value is chosen too small, i.e., $\varepsilon < \varepsilon_{opt}$.

Finally, we consider the computational time presented in Figure 6.5. We note that the CPU time needed for the exact strategy (RM=3) is *much* higher as long as the threshold value is not too small. This is caused by the source term computation

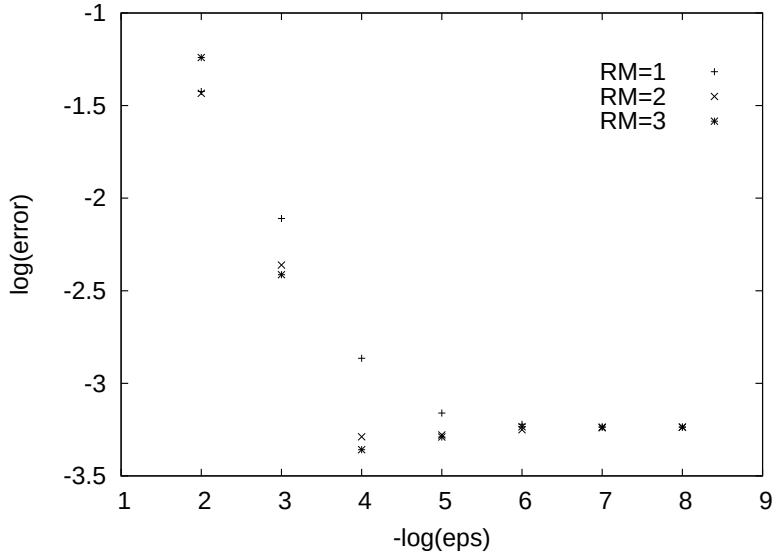


FIG. 6.3. *Error of adaptive solution with $L = 10$ and varying threshold value $\varepsilon$.*

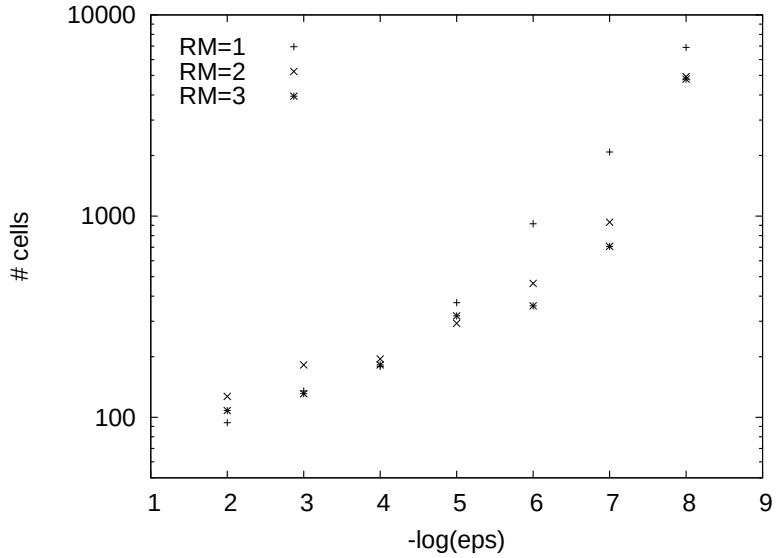


FIG. 6.4. *Number of cells: Adaptive computations with $L = 10$ and varying threshold value $\varepsilon$.*

on the uniform reference grid dominating the overall costs for grid adaptation and time evolution. In case of the local (RM=1) and approximate (RM=2) strategy the adaptive grid becomes more dense with decreasing threshold values, i.e., more cells are refined, and the costs are approaching the costs of the reference computation on the reference grid. This behaviour can be typically expected for any adaptive scheme.

To summarize the above observations we conclude that for an optimal threshold value $\varepsilon_{opt}$ the exact strategy is most accurate but at the costs of the reference computation, i.e., there is no gain at all. For the local strategy we observe a severe loss

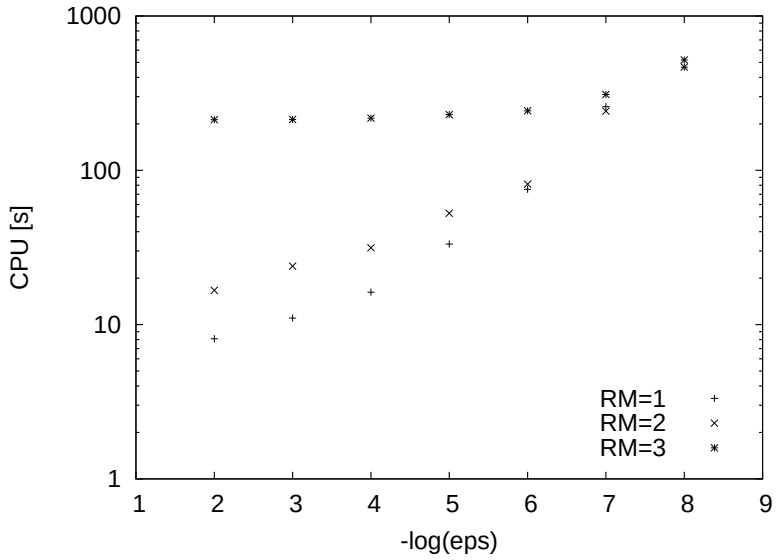


FIG. 6.5. *Computational time: Adaptive computations with $L = 10$ and varying threshold value $\varepsilon$.*

in accuracy at lower computational costs in comparison to the approximate strategy. This loss can only be compensated by a smaller threshold value at higher computational costs. From this point of view the approximate strategy is more efficient when fixing the target accuracy by the discretization error, i.e., $\log(\|\boldsymbol{\tau}_L\|) = -3.24$, see Figure 6.6.

Finally, we point out that in practice the optimal threshold value $\varepsilon_{opt}$ can only be roughly estimated and, hence, the use of the local strategy can not be recommended because we either (i) are loosing significant in accuracy if $\varepsilon \gg \varepsilon_{opt}$, see Figures 6.3, or (ii) the computational costs (memory requirements) are significantly higher due to instabilities triggered by the increasing influence of the reconstruction error if $\varepsilon \ll \varepsilon_{opt}$, see Figure 6.4.

**Acknowledgments.** The authors would like to thank their colleague Dr. Philipp Lamby for careful proof-reading and many valuable remarks.

## REFERENCES

[1] R. Abgrall. Multiresolution analysis on unstructured meshes: Applications to CFD. In Chetverushkin et al., editor, *Experimentation, modelling and computation in flow, turbulence and combustion*. John Wiley & Sons, 1997.

[2] F. Arandiga, R. Donat, and A. Harten. Multiresolution based on weighted averages of the hat function I: Linear reconstruction techniques. *SIAM J. Numer. Anal.*, 36(1):160–203, 1998.

[3] B. Bihari and A. Harten. Multiresolution schemes for the numerical solution of 2–D conservation laws I. *SIAM J. Sci. Comput.*, 18(2):315–354, 1997.

[4] F. Bramkamp, Ph. Lamby, and S. Müller. An adaptive multiscale finite volume solver for unsteady an steady state flow computations. *J. Comp. Phys.*, 197(2):460 –490, 2004.

[5] J.M. Carnicer, W. Dahmen, and J.M. Peña. Local decomposition of refinable spaces and wavelets. *Appl. Comput. Harmon. Anal.*, 3:127–153, 1996.

[6] G. Chiavassa, R. Donat, and S. Müller. Multiresolution-based adaptive schemes for hyperbolic conservation laws. In T. Plewa et al., editor, *Adaptive mesh refinement – theory and applications*, volume 41 of *Lecture Notes on Computational Science and Engineering*, pages 137–159. Berlin: Springer, 2005.

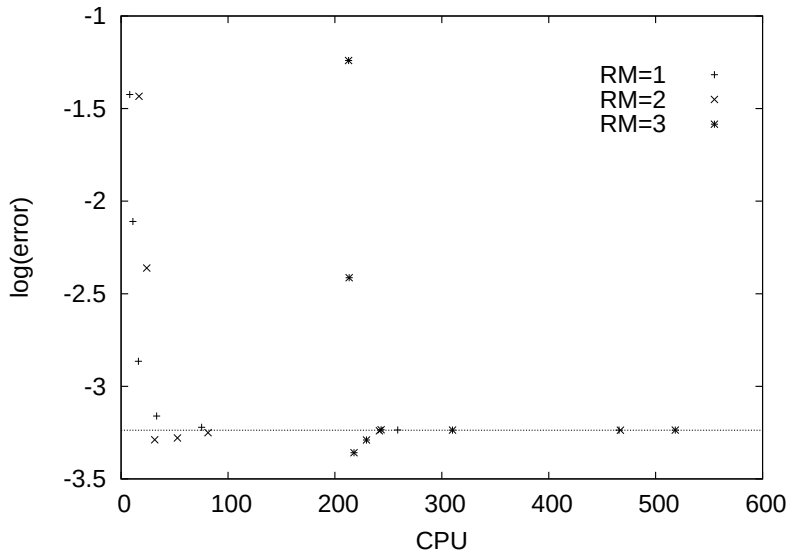


FIG. 6.6. *Comparison of CPU time and error of adaptive scheme for different threshold values.*

[7] A. Cohen. Wavelet Methods in Numerical Analysis. In P.G. Ciarlet and J.L. Lions, editors, *Handbook of Numerical Analysis*, Handbook of Numerical Analysis, pages 417–711. Elsevier, Amsterdam, 2000.

[8] A. Cohen, N. Dyn, S.M. Kaber, and M. Postel. Multiresolution finite volume schemes on triangles. *J. Comp. Physics*, 161:264–286, 2000.

[9] A. Cohen, S.M. Kaber, S. Müller, and M. Postel. Fully Adaptive Multiresolution Finite Volume Schemes for Conservation Laws. *Math. Comp.*, 72(241):183–225, 2003.

[10] W. Dahmen, B. Gottschlich–Müller, and S. Müller. Multiresolution schemes for conservation laws. *Numer. Math.*, 88(3):399–443, 2000.

[11] E. Godlewski and P.-A. Raviart. *Hyperbolic systems of conservation laws.* Mathématiques & Applications (Paris). 3-4. Paris: Ellipses, 252 p., 1991.

[12] B. Gottschlich–Müller and S. Müller. Adaptive finite volume schemes for conservation laws based on local multiresolution techniques. In M. Fey and R. Jeltsch, editors, *Hyperbolic Problems: Theory, Numerics, Applications*, pages 385–394. Birkhäuser, 1999.

[13] A. Harten. Multiresolution algorithms for the numerical solution of hyperbolic conservation laws. *Comm. Pure Appl. Math.*, 48(12):1305–1342, 1995.

[14] A. Harten. Multiresolution representation of data: A general framework. *SIAM J. Numer. Anal.*, 33(3):1205–1256, 1996.

[15] A. Harten, B. Engquist, S. Osher, and S.R. Chakravarthy. Uniformly high order accurate essentially non–oscillatory schemes III. *J. Comp. Phys.*, 71:231–303, 1987.

[16] M. K. Kaibara and S. M. Gomes. A fully adaptive multiresolution scheme for shock computations. In E. F. Toro, editor, *Godunov methods. Theory and applications*, pages 497–503. New York, NY: Kluwer Academic/ Plenum Publishers, 2001.

[17] S. N. Kruzhkov. First order quasilinear equations in several independent variables. *Math. USSR Sbornik*, 10:217–243, 1970.

[18] S. Müller. *Adaptive Multiscale Schemes for Conservation Laws*, volume 27 of *Lecture Notes on Computational Science and Engineering*. Springer, 2002.

[19] O. A. Oleinik. Discontinuous solutions of nonlinear differential equations. *Amer. Math. Soc. Transl. Ser. 2*, 26:95–172, 1963.

[20] A. Rault, G. Chiavassa, and R. Donat. Shock-vortex interactions at high Mach numbers. *J. Scientific Computing*, 19:347–371, 2003.

[21] O. Roussel, K. Schneider, A. Tsigulin, and H. Bockhorn. A conservative fully adaptive multiresolution algorithm for parabolic PDEs. *J. Comp. Phys.*, 188(2):493–523, 2003.

[22] W. Sweldens. The lifting scheme: A construction of second generation wavelets. *SIAM J. Math. Anal.*, 29(2):511–546, 1998.

## 7. Appendix.

### 7.1. Proof of Lemma 5.3.

*Proof.* In order to estimate the extrema by the time evolution we consider

$$\begin{aligned}\|\check{\mathbf{v}}_L^n\|_{l^\infty} \le\ & \|\mathcal{A}_\varepsilon\, \check{\mathcal{E}}_{L,\bar{\mathcal{D}}^n}\, \mathcal{A}_{\bar{\mathcal{D}}^n}\, \check{\mathbf{v}}_L^{n-1} - \check{\mathcal{E}}_{L,\bar{\mathcal{D}}^n}\, \mathcal{A}_{\bar{\mathcal{D}}^n}\, \check{\mathbf{v}}_L^{n-1}\|_{l^\infty} + \\ & \|\check{\mathcal{E}}_{L,\bar{\mathcal{D}}^n}\, \mathcal{A}_{\bar{\mathcal{D}}^n}\, \check{\mathbf{v}}_L^{n-1} - \bar{\mathcal{E}}_{L,\bar{\mathcal{D}}^n}\, \mathcal{A}_{\bar{\mathcal{D}}^n}\, \check{\mathbf{v}}_L^{n-1}\|_{l^\infty} + \\ & \|\bar{\mathcal{E}}_{L,\bar{\mathcal{D}}^n}\, \mathcal{A}_{\bar{\mathcal{D}}^n}\, \check{\mathbf{v}}_L^{n-1} - \mathcal{E}_L\, \check{\mathbf{v}}_L^{n-1}\|_{l^\infty} + \|\mathcal{E}_L \check{\mathbf{v}}_L^{n-1}\|_{l^\infty} \end{aligned} \tag{7.1}$$

By the definition of the approximation error the first term can be estimated according to (2.11) by

$$\|\mathcal{A}_\varepsilon\, \check{\mathcal{E}}_{L,\bar{\mathcal{D}}^n}\, \mathcal{A}_{\bar{\mathcal{D}}^n}\, \check{\mathbf{v}}_L^{n-1} - \check{\mathcal{E}}_{L,\bar{\mathcal{D}}^n}\, \mathcal{A}_{\bar{\mathcal{D}}^n}\, \check{\mathbf{v}}_L^{n-1}\|_{l^\infty} \le \left\| \sum_{l=0}^{L-1} \sum_{k\in\mathcal{J}_{l,\varepsilon}^n} \check{d}_{l,k}^{n-1}\, \mathbf{\Psi}_{l,k}^L \right\|_{l^\infty},$$

where $\mathcal{J}_{l,\varepsilon}^n$ indicates the non-significant details on level $l$. It should be noted that $\tilde{\mathcal{D}}^\nu$ is computed from the data of the modified adaptive scheme at the old time step, i.e., $\check{\mathbf{v}}_L^{\nu-1}$. Reliability then means

$$\|\mathcal{A}_{\bar{\mathcal{D}}^\nu}\, \mathcal{E}_L\, \check{\mathbf{v}}_L^{\nu-1}\|_{l^\infty} \le C\varepsilon.$$

From assumption (A6) and Theorem 2.1 we conclude that the supports of the discrete basis vectors $\mathbf{\Psi}_{l,k}^L$ overlap only at a fixed number of positions independent of $l$ and $k$. This implies

$$\left\| \sum_{k\in\mathcal{J}_{l,\varepsilon}^n} \check{d}_{l,k}^{n-1}\, \mathbf{\Psi}_{l,k}^L \right\|_{l^\infty} \le \sup_{k\in\mathcal{J}_{l,\varepsilon}^n} |\check{d}_{l,k}^{n-1}|\, \left\|\psi_{l,k}^L\right\|_{L^\infty} \le C\, \varepsilon_l, \tag{7.2}$$

where we employ that the prediction set is reliable in the sense of (3.7). Thus the first term can be estimated by

$$\|\mathcal{A}_\varepsilon\, \check{\mathcal{E}}_{L,\bar{\mathcal{D}}^n}\, \mathcal{A}_{\bar{\mathcal{D}}^n}\, \check{\mathbf{v}}_L^{n-1} - \check{\mathcal{E}}_{L,\bar{\mathcal{D}}^n}\, \mathcal{A}_{\bar{\mathcal{D}}^n}\, \check{\mathbf{v}}_L^{n-1}\|_{l^\infty} \le \sum_{l=0}^{L-1} \varepsilon_l \le C\, \varepsilon.$$

The second term is estimated according to the assumption (A7). Due to (5.3) the third term can be rewritten

$$\bar{\mathcal{E}}_{L,\bar{\mathcal{D}}^n}\, \mathcal{A}_{\bar{\mathcal{D}}^n} = \mathcal{A}_{\bar{\mathcal{D}}^n}\, \mathcal{E}_L.$$

Then the difference can be estimated by the approximation property as above

$$\|\bar{\mathcal{E}}_{L,\bar{\mathcal{D}}^n}\, \mathcal{A}_{\bar{\mathcal{D}}^n}\, \check{\mathbf{v}}_L^{n-1} - \mathcal{E}_L\, \check{\mathbf{v}}_L^{n-1}\|_{l^\infty} = \|\mathcal{A}_{\bar{\mathcal{D}}^n}\, \mathcal{E}_L \check{\mathbf{v}}_L^{n-1} - \mathcal{E}_L\, \check{\mathbf{v}}_L^{n-1}\|_{l^\infty} \le \varepsilon, \tag{7.3}$$

where we employ the reliability of $\tilde{\mathcal{D}}^n$.

The fourth term can be estimated according to (A8) by

$$\|\mathcal{E}_L\, \check{\mathbf{v}}_L^{n-1}\|_{l^\infty} \le (1 + C\,\tau)\, \|\check{\mathbf{v}}_L^{n-1}\|_{l^\infty}.$$

From (7.1) we finally obtain the recursive estimate

$$\|\check{\mathbf{v}}_L^n\|_{l^\infty} \leq (1 + C\,\tau)\,\|\check{\mathbf{v}}_L^{n-1}\|_{l^\infty} + \bar{C}\varepsilon.$$

Applying this estimate recursively, we obtain

$$\|\check{\mathbf{v}}_L^n\|_{l^\infty} \leq (1 + C\,\tau)^n\,\|\check{\mathbf{v}}_L^0\|_{l^\infty} + \bar{C}\,\varepsilon \sum_{i=0}^{n-1} (1 + C\,\tau)^i.$$

By the geometric sum we finally end up with

$$\|\check{\mathbf{v}}_L^n\|_{l^\infty} \leq e^{C\,T}\,\|\check{\mathbf{v}}_L^0\|_{l^\infty} + \bar{C}\,\varepsilon \frac{(1 + C\,\tau)^n - 1}{C\,\tau} \leq e^{C\,T}\,(\|\check{\mathbf{v}}_L^0\|_{l^\infty} + \bar{\bar{C}}\,\varepsilon/\tau).$$

The initial data can be further estimated

$$\|\check{\mathbf{v}}_L^0\|_{l^\infty} \leq \|\hat{\mathbf{u}}_L^0\|_{l^\infty} + \|\check{\mathbf{v}}_L^0 - \mathbf{v}_L^0\|_{l^\infty} + \|\mathbf{v}_L^0 - \hat{\mathbf{u}}_L^0\|_{l^\infty} \leq \|u_0\|_{L^\infty} + 2\,\check{C}\,\varepsilon/\tau.$$

From assumption (A10) and (A11) we conclude that the ratio $\varepsilon/\tau$ is small in comparison to $\|u_0\|_{L^\infty}$. Consequently, we can estimate the supremum of $\check{\mathbf{v}}_L^n$ by a constant only depending on $T$ and the supremum of the initial data $u_0$. ∎

### 7.2. Proof of Lemma 5.10.

*Proof.* The average of the reconstruction polynomial is determined by

$$\hat{P}_r = \frac{1}{h}\int_{x_r}^{x_{r+1}} \frac{d}{dx} Q_k^{N+1}(x)\,dx = \frac{1}{h}\left(Q_k^{N+1}(x_{r+1}) - Q_k^{N+1}(x_r)\right)$$

for any $r \in \mathbb{Z}$. Then $\Delta_1^{N+1}\hat{P}_r$ can be interpreted as the difference of finite differences of the interpolation polynomial $Q_k^{N+1}$, i.e.,

$$\begin{aligned}\Delta_1^{N+1}\hat{P}_r = \sum_{i=0}^{N+1} (-1)^i \binom{N+1}{i} \hat{P}_{r+i} = \\ \frac{1}{h}\sum_{i=0}^{N+1} (-1)^i \binom{N+1}{i} \left(Q_k^{N+1}(x_{r+i+1}) - Q_k^{N+1}(x_{r+i})\right) = \\ \frac{1}{h}\left(\Delta_1^{N+1} Q_k^{N+1}(x_{r+1}) - \Delta_1^{N+1} Q_k^{N+1}(x_r)\right).\end{aligned}$$

Since $Q_k^{N+1} \in \Pi_{N+1}$ the finite difference satisfies

$$\Delta_1^{N+1} Q_k^{N+1}(x) = \frac{h^{N+1}}{(N+1)!}\frac{d^{N+1}}{dx^{N+1}} Q_k^{N+1}(\zeta) = \text{const}, \quad \zeta \in [x_{\underline{k}}, x_{\overline{k}+1}],$$

therefore

$$\Delta_1^{N+1}\hat{P}_r = 0, \qquad \forall r \in \mathbb{Z}. \tag{7.4}$$

We will use these considerations in the following.

In order to verify that the difference $v_{k'} - \hat{P}_{k'}$ for $k' \notin \mathcal{S}_k$ can be written in the form of a finite sum of finite differences of order $N+1$ we use the induction principle for $k' < \underline{k}$.

First, we consider the case $k' = \underline{k} - 1$. According to the reconstruction condition (5.24) we obtain

$$v_{\underline{k}-1} - \hat{P}_{\underline{k}-1} = \Delta_1^{N+1} v_{\underline{k}-1} - \sum_{r=1}^{N} (-1)^r \binom{N+1}{r} v_{\underline{k}-1+r} - \hat{P}_{\underline{k}-1} = \Delta_1^{N+1} v_{\underline{k}-1} - \Delta_1^{N+1} \hat{P}_{\underline{k}-1}.$$

Taking into account (7.4) we have got

$$v_{\underline{k}-1} - \hat{P}_{\underline{k}-1} = \Delta_1^{N+1} v_{\underline{k}-1}.$$

Therefore our assertion is true for $k' = \underline{k}-1$. Let it be true for $k' \in \{\underline{k}-N_s, \ldots, \underline{k}-1\}$, $N_s \geq 1$. We now prove it for $k'-1$ and $N_s+1$, respectively. For this purpose we expand the difference as

$$v_{k'-1} - \hat{P}_{k'-1} = \Delta_1^{N+1} v_{k'-1} - \Delta_1^{N+1} \hat{P}_{k'-1} - \sum_{r=1}^{N+1} \binom{N+1}{r} (-1)^r (v_{k'-1+r} - \hat{P}_{k'-1+r}),$$

where we employ the definition of the finite difference. For $k'-1+r \in \mathcal{S}_k$ the differences in the sum of the right-hand side vanish, i.e., only the differences for $r \in \{1, \ldots, \min(N+1, \underline{k}-k')\}$ give a contribution.

Since the $(N+1)$-th finite difference of $\hat{P}$ vanishes according to (7.4) and by the induction assumption

$$v_{k'-1+r} - \hat{P}_{k'-1+r} = \sum_{j=0}^{\underline{k}-k'-r} \alpha_{k'-1+r,j} \Delta_1^{N+1} v_{k'-1+r+j} \tag{7.5}$$

for $r \in \{1, \ldots, \min(N+1, \underline{k}-k')\}$ we then conclude

$$v_{k'-1} - \hat{P}_{k'-1} = \Delta_1^{N+1} v_{k'-1} + \sum_{r=1}^{\min(N+1, \underline{k}-k')} \binom{N+1}{r} (-1)^{r+1} \sum_{j=0}^{\underline{k}-k'-r} \alpha_{k'-1+r,j} \Delta_1^{N+1} v_{k'-1+r+j}.$$

Since $k'-1+r+j \in \{k', \ldots, \underline{k}-1\}$ the right-hand side can be reenumerated, i.e.,

$$v_{k'-1} - \hat{P}_{k'-1} = \sum_{j=0}^{\underline{k}-k'} \alpha_{k'-1,j} \Delta_1^{N+1} v_{k'-1+j}.$$

Hence we obtain the assertion for $k' < \underline{k}$.

We now prove the other case where $k'$ is to the right of $\mathcal{S}_{l,k}$. Again, we first consider the case $k' = \overline{k}+1$. According to (5.24) and (7.4) we have

$$\begin{aligned} v_{\overline{k}+1} - \hat{P}_{\overline{k}+1} &= (-1)^{N+1} \Delta_1^{N+1} v_{\underline{k}} - (-1)^{N+1} \sum_{r=0}^{N} (-1)^r \binom{N+1}{r} v_{\underline{k}+r} - \hat{P}_{\overline{k}+1} \\ &= (-1)^{N+1} \left( \Delta_1^{N+1} v_{\underline{k}} - \Delta_1^{N+1} \hat{P}_{\underline{k}} \right) = (-1)^{N+1} \Delta_1^{N+1} v_{\underline{k}}. \end{aligned}$$

Therefore our assertion is true for $k' = \overline{k}+1$. Let it be true for $k' \in \{\overline{k}+1, \ldots, \overline{k}+N_s\}$, $1 \leq N_s$. We now prove it for $k'+1$ and $N_s+1$, respectively. For this purpose we

expand the difference as

$$v_{k'+1} - \hat{P}_{k'+1} =$$
$$(-1)^{N+1}\left(\left(\Delta_1^{N+1} v_{k'-N} - \Delta_1^{N+1}\hat{P}_{k'-N}\right) - \sum_{r=0}^{N}\binom{N+1}{r}(-1)^r(v_{k'-N+r} - \hat{P}_{k'-N+r})\right)$$

where we again employ the definition of the finite difference. For $k' - N + r \in \mathcal{S}_k$ the differences in the sum of the right-hand side vanish, i.e., only the differences for $r \in \{\max(0, \overline{k} - k' + N + 1), \dots, N\}$ give a contribution. Since the $(N+1)$-st finite difference of $\hat{P}$ vanishes according to (7.4) and by the induction assumption

$$v_{k'-N+r} - \hat{P}_{k'-N+r} = \sum_{j=0}^{k'-N+r-\overline{k}-1} \alpha_{k'-N+r,j}\Delta_1^{N+1} v_{k'-2N+r-j-1},$$

for $r \in \{\max(0, \overline{k} - k' + N + 1), \dots, N\}$ we then conclude

$$v_{k'+1} - \hat{P}_{k'+1} = (-1)^{N+1}\Bigg(\Delta_1^{N+1} v_{k'-N} +$$
$$\sum_{r=\max(0,\overline{k}-k'+N+1)}^{N}\binom{N+1}{r}(-1)^{r+1}\sum_{j=0}^{k'-N+r-\overline{k}-1}\alpha_{k'-N+r,j}\Delta_1^{N+1} v_{k'-2N+r-j-1}\Bigg).$$

Since $k' - 2N + r - j - 1 \in \{\overline{k} - N, \dots, k' - N - 1\}$ the right-hand side can be reenumerated, i.e.,

$$v_{k'+1} - \hat{P}_{k'+1} = \sum_{j=0}^{k'-\overline{k}} \alpha_{k'+1,j}\Delta_1^{N+1} v_{k'-N-j}.$$

□

### 7.3. Proof of Lemma 5.11.

*Proof.* For $N = 1$ we obtain by the two-scale relation (2.3)

$$\Delta_1^1 v_{l,k} = v_{l,k} - v_{l,k+1} = \frac{1}{2}(v_{l+1,2k} + v_{l+1,2k+1} - v_{l+1,2k+2} - v_{l+1,2k+3}) =$$
$$\frac{1}{2}(v_{l+1,2k} - v_{l+1,2k+1} + 2(v_{l+1,2k+1} - v_{l+1,2k+2}) + v_{l+1,2k+2} - v_{l+1,2k+3}) =$$
$$\frac{1}{2}(\Delta_1^1 v_{l+1,2k} + 2\Delta_1^1 v_{l+1,2k+1} + \Delta_1^1 v_{l+1,2k+2}) = \frac{1}{2}\sum_{i=0}^{2}\binom{2}{i}\Delta_1^1 v_{l+1,2k+i}. \tag{7.6}$$

Assume now that the assertion (5.25) holds for $N$. To prove it for $N+1$ we first note that by the standard recursive definition of finite differences

$$\Delta_1^{N+1} v_{l,k} = \Delta_1^N v_{l,k} - \Delta_1^N v_{l,k+1} \tag{7.7}$$

holds. Then we obtain by the induction assumption

$$\Delta_1^{N+1} v_{l,k} = \frac{1}{2}\left(\sum_{i=0}^{N+1}\binom{N+1}{i}\Delta_1^N v_{l+1,2k+i} - \sum_{i=0}^{N+1}\binom{N+1}{i}\Delta_1^N v_{l+1,2k+2+i}\right).$$

Adding and subtracting $\Delta_1^N v_{l+1,2k+i}$ and applying (7.7) for $(l+1, 2k+i)$ and $(l+1, 2k+1+i)$ yields

$$\begin{aligned}\Delta_1^{N+1} v_{l,k} &= \frac{1}{2}\left(\sum_{i=0}^{N+1}\binom{N+1}{i}(\Delta_1^N v_{l+1,2k+i} - \Delta_1^N v_{l+1,2k+1+i}) + \right.\\ &\qquad \left.\sum_{i=0}^{N+1}\binom{N+1}{i}(\Delta_1^N v_{l+1,2k+1+i} - \Delta_1^N v_{l+1,2k+2+i})\right)\\ &= \frac{1}{2}\left(\sum_{i=0}^{N+1}\binom{N+1}{i}\Delta_1^{N+1} v_{l+1,2k+i} + \sum_{i=0}^{N+1}\binom{N+1}{i}\Delta_1^{N+1} v_{l+1,2k+1+i}\right).\end{aligned}$$

Similar to (7.6) we verify by means of the addition theorem for binomial coefficients

$$\begin{aligned}&\Delta_1^{N+1} v_{l,k} = \\ &\frac{1}{2}\left(\Delta_1^{N+1} v_{l+1,2k} + \sum_{i=1}^{N+1}\left(\binom{N+1}{i} + \binom{N+1}{i-1}\right)\Delta_1^{N+1} v_{l+1,2k+i} + \Delta_1^{N+1} v_{l+1,2k+N+2}\right)\\ &= \frac{1}{2}\sum_{i=0}^{N+2}\binom{N+2}{i}\Delta_1^{N+1} v_{l+1,2k+i}.\end{aligned}$$

This proves (5.25). To verify (5.26) we only have to do a straight-forward calculation using the encoding (2.3) and the definition (5.10) of the finite difference, i.e.,

$$\begin{aligned}&\Delta_1^N v_{l,k} \overset{(5.10)}{=} \sum_{i=0}^{N}\binom{N}{i}(-1)^i v_{l,k+i} \overset{(2.3)}{=} \sum_{i=0}^{N}\binom{N}{i}(-1)^i 2^{l-L}\sum_{\nu=0}^{2^{L-l}-1} v_{L,2^{L-l}(k+i)+\nu} =\\ &2^{l-L}\sum_{\nu=0}^{2^{L-l}-1}\sum_{i=0}^{N}\binom{N}{i}(-1)^i v_{L,2^{L-l}k+\nu+2^{L-l}i} \overset{(5.10)}{=} 2^{l-L}\sum_{\nu=0}^{2^{L-l}-1}\Delta_{2^{L-l}}^N v_{L,2^{L-l}k+\nu}.\end{aligned}$$

□

### 7.4. Proof of Lemma 5.12.

*Proof.* By means of (5.25) the finite differences are represented by those on one higher level with step size 1, i.e.,

$$\Delta_1^{N+1} v_{l,k'} = \frac{1}{2}\sum_{i=0}^{N+2}\binom{N+2}{i}\Delta_1^{N+1} v_{l+1,2k'+i} \tag{7.8}$$

and then the finite differences on the right-hand side are represented by those on level $L$ with step size $2^{L-l-1}$ using (5.26), i.e.,

$$\Delta_1^{N+1} v_{l+1,2k'+i} = 2^{l+1-L}\sum_{\mu=0}^{2^{L-l-1}-1}\Delta_{2^{L-l-1}}^{N+1} v_{L,2^{L-l-1}(2k'+i)+\mu}. \tag{7.9}$$

Note that we cannot directly apply (5.26) to $\Delta_1^{N+1} v_{l,k'}$ because the step size $2^{L-l}$ will be too large and we are running into trouble when want to apply Lemma 5.7.

In view of Lemma 5.7 we now have to verify for each finite difference on the right-hand side of (7.8) that its stencil (5.11)

$$S\left(N+1, 2^{L-l-1}, 2^{L-l-1}(2k'+i)+\mu\right) = \{2^{L-l-1}(2k'+i)+\mu, \dots, 2^{L-l-1}(2k'+i+N+1)+\mu\} \quad (7.10)$$

is included in a backward influence set (5.6)

$$\tilde{\Sigma}^{-}_{l+1,2k+q',1} = \{2^{L-l-1}(2k+q'-s)-p, \dots, 2^{L-l-1}(2k+q'+s+1)-1+p\} \quad (7.11)$$

for some $q'$ such that $(l+1, 2k+q') \notin \mathcal{D}$, i.e.,

$$S\left(N+1, 2^{L-l-1}, 2^{L-l-1}(2k'+i)+\mu\right) \subset \tilde{\Sigma}^{-}_{l+1,2k+q',1} \quad (7.12)$$

holds for any $\mu \in \{0, \dots, 2^{L-l-1}-1\}$. In fact, $q'$ is related to the grading parameter in the grading procedure (3.11). To verify the inclusion (7.12) the following conditions have to hold according to (7.10) and (7.11)

$$\begin{aligned} &2k+q'-s-p\,2^{l+1-L} \le 2k'+i+2^{l+1-L}\mu, \\ &2k'+i+N+1+2^{l+1-L}\mu \le 2k+q'+s+1-2^{l+1-L}(1-p). \end{aligned}$$

This is equivalent to

$$2(k'-k)+i+N-s+2^{l+1-L}(\mu+1-p) \le q \le 2(k'-k)+i+s+2^{l+1-L}(\mu+p).$$

Obviously this inequality holds true for

$$q' := \begin{cases} 2(k'-k)+i+s+\mu 2^{l+1-L}, & k' \in \{k-2s, \dots, k-1\}, \\ 2(k'-k)+i+N-s+\mu 2^{l+1-L}, & k' \in \{k-N, \dots, k+2s-N-1\}, \end{cases}$$

because $N \le 2s$ and $p \ge 1$. Since $i \in \{0, \dots, N+2\}$, $\mu \in \{0, \dots, 2^{L-l-1}-1\}$ and $k-k' \in \{1, \dots, 2s\}$ for $k' \in \{k-2s, \dots, k-1\}$ and $k'-k \in \{-N, \dots, 2s-N-1\}$ for $k' \in \{k-N, \dots, k+2s-N-1\}$ we conclude

$$q' \in \{-3s, \dots, 3s+1\}$$

and, hence,

$$2k+q' \in \{2k-3s, \dots, 2k+3s+1\} = \left\{2\left(k-\frac{3s}{2}\right), \dots, 2\left(k+\frac{3s+1}{2}\right)\right\}.$$

On the other hand we know by the grading procedure and the assumption $(l,k) \in \mathcal{G}$, i.e., $(l,k) \notin \mathcal{D}$, that all details corresponding to the range of dependence given by

$$\tilde{\Sigma}^{\mathcal{G},(j)}_{l,k} = \{2^{j-l}(k-q), \dots, 2^{j-l}(k+q+1)-1\}, \quad j = l+1, \dots, L-1,$$

are non-significant. In particular, for $j = l+1$ we obtain the range of dependence for $(l,k)$ on level $l+1$

$$\tilde{\Sigma}^{\mathcal{G},(l+1)}_{l,k} = \{2(k-q), \dots, 2(k+q)+1\}.$$

To ensure that $2k+q' \in \tilde{\Sigma}^{\mathcal{G},(l+1)}_{l,k}$ we have to choose the grading parameter $q$ such that

$$2(k-q) \le 2\left(k-\frac{3s}{2}\right) \quad \text{and} \quad 2\left(k+\frac{3s+1}{2}\right) \le 2(k+q)+1.$$

Obviously it holds by assumption.

Since for any $i \in \{0,\dots,N+2\}$ and $\mu \in \{0,\dots,2^{L-l-1}-1\}$ there exists $q'$ such that $(l+1, 2k+q') \notin \mathcal{D}$ and (7.12) holds true, we may apply Lemma 5.7, i.e.,

$$\left|\Delta^{N+1}_{2^{L-l-1}} v_{L,2^{L-l-1}(2k'+i)+\mu}\right| \lesssim \varepsilon_{l+1}^{\min\left(\frac{N+1}{R},1\right)}.$$

Together with (7.9) this implies

$$\left|\Delta^{N+1}_{1} v_{l+1,2k'+i}\right| \lesssim \varepsilon_{l+1}^{\min\left(\frac{N+1}{R},1\right)}.$$

Finally we conclude from (7.8)

$$\left|\Delta^{N+1}_{1} v_{l,k'}\right| \lesssim \varepsilon_{l}^{\min\left(\frac{N+1}{R},1\right)}.$$

Note that $\varepsilon_{l+1} = 2\varepsilon_l$ and $\sum_{i=0}^{N+2}\binom{N+2}{i} = 2^{N+2}$ is independent of the level. ∎

### 7.5. Proof of Lemma 5.13.

*Proof.* First of all we introduce the fine-scale cell averages of the reconstruction polynomial $R^N_{l,k}$, i.e.,

$$\hat{P}_{L,r} := \frac{1}{|V_{L,r}|}\int_{V_{L,r}} R^N_{l,k}(x)\,dx = \langle R^N_{l,k}, \tilde{\varphi}_{L,r}\rangle, \quad r \in I_L.$$

Since $M \geq N+1$ the corresponding details vanish, i.e.,

$$d^P_{j,r} := \langle R^N_{l,k}, \tilde{\psi}_{j,r}\rangle = 0, \quad j = 0,\dots,L-1,\ r \in I_j.$$

Applying the subdivision scheme (2.8) to $\hat{P}_{L,r}$ we obtain for $r \in I_L$

$$\hat{P}_{L,r} = \sum_{k' \in \bar{\Sigma}^{(l)}_{L,r,0}} \left(\mathbf{\Psi}^L_{l,k',0}\right)_r \hat{P}_{l,k'} = \sum_{k' \in \mathcal{S}_{l,k}} \left(\mathbf{\Psi}^L_{l,k',0}\right)_r v_{l,k'} + \sum_{k' \in \bar{\Sigma}^{(l)}_{L,r,0}\setminus\mathcal{S}_{l,k}} \left(\mathbf{\Psi}^L_{l,k',0}\right)_r \hat{P}_{l,k'}. \tag{7.13}$$

On the other hand we may write the data $\mathbf{v}_L$ by the subdivision scheme (2.8) as

$$v_{L,r} = \sum_{k' \in \bar{\Sigma}^{(l)}_{L,r,0}} \left(\mathbf{\Psi}^L_{l,k',0}\right)_r v_{l,k'} + \sum_{j=l}^{L-1}\sum_{k' \in \bar{\Sigma}^{(j)}_{L,r,1}} \left(\mathbf{\Psi}^L_{j,k',1}\right)_r d_{j,k'}. \tag{7.14}$$

We now confine ourselves to $r \in \{2^{L-l}k,\dots,2^{L-l}(k+1)-1\}$. Then we obtain for the support of the subdivision scheme (2.8) the inclusion

$$\bar{\Sigma}^{(j)}_{L,r,1} \subset \{\lfloor r/2^{L-j}\rfloor - s,\dots,\lfloor r/2^{l-j}\rfloor + s\}$$

for $j = l,\dots,L-1$. Hence

$$\bar{\Sigma}^{(j)}_{L,r,1} \subset \{2^{j-l}k - s,\dots,2^{j-l}k + s\}, \quad j = l,\dots,L-1.$$

On the other hand, $(l,k) \in \mathcal{G}$ according to assumption and therefore $(l,k) \notin \mathcal{D}$, i.e., $d_{lk} = 0$, otherwise $V_{l,k}$ would have been refined by the grid refinement procedure. Then all details in the range of dependence

$$\tilde{\Sigma}^{\mathcal{G},(j)}_{l,k} = \{2^{j-l}(k-q),\dots,2^{j-l}(k+q+1)-1\}, \quad j = l+1,\dots,L-1, \tag{7.15}$$

are not significant either, otherwise $(l,k)$ would be put significant by the grading procedure.

Assuming that $q \geq s$ we conclude that the support of the wavelets $\bar{\Sigma}^{(j)}_{L,r,1}$ is included in the range of dependence $\tilde{\Sigma}^{\mathcal{G},(j)}_{l,k}$ for all $r \in \{2^{L-l}k, \dots, 2^{L-l}(k+1)-1\}$ and $j = l+1, \dots, L-1$, see Fig. 7.1. Then (7.14) reduces to

$$v_{L,r} = \sum_{k' \in \bar{\Sigma}^{(l)}_{L,r,0}} \left(\mathbf{\Psi}^L_{l,k',0}\right)_r v_{l,k'} + \sum_{k' \in \bar{\Sigma}^{(l)}_{L,r,1} \setminus \{k\}} \left(\mathbf{\Psi}^L_{l,k',1}\right)_r d_{l,k'}. \tag{7.16}$$

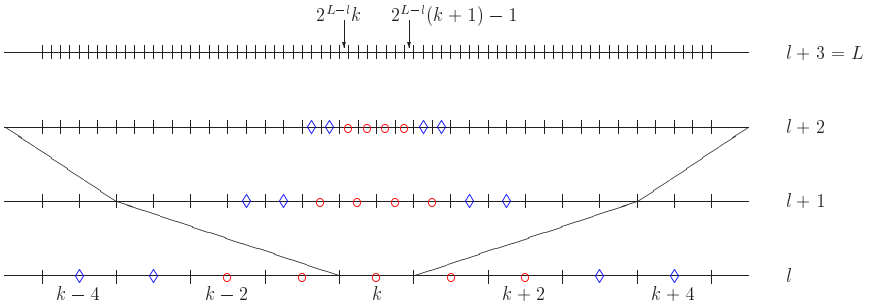


FIG. 7.1. *Illustration of the cell averages (◇ and ○) and the details (○) involved in the subdivision scheme of any cell average $v_{L,r}$, $r = 2^{L-l}k, \dots, 2^{L-l}(k+1)-1$ with $s=2$. The range of dependence for the detail corresponding to cell $(l,k)$ is bounded by the oblique lines. Here we assume that the set of significant details is a graded tree of degree $q = \lceil \frac{3s}{2} \rceil = 3$ with $s=2$.*

Now consider the remaining details $d_{l,k'}$ for $k' \in \bar{\Sigma}^{(l)}_{L,r,1} \subset \{k-s, \dots, k+s\}$. The details on the higher levels $d_{l+1,2k'+i}$, $i=0,1$ can not be significant. Otherwise, $(l,k) \in \mathcal{D}$ due to the grading and $q \geq s$. According to the definition of the prediction set (5.8) we infer that $\nu(l,k') = 0$. Hence we can estimate the details due to the nesting of (5.7) by

$$|d_{l,k'}| \leq 2^{\sigma} \varepsilon_l, \tag{7.17}$$

where $\sigma$ is a constant which is fixed in Assumption 2.

Next we have to estimate the differences of the cell averages $v_{l,k'}$ and $\hat{P}_{l,k'}$ for $k' \in \bar{\Sigma}^{(l)}_{L,r,0} \setminus \mathcal{S}_{l,k}$. For this purpose we will apply Lemmas 5.10 and 5.11. First of all, we note that the support $\bar{\Sigma}^{(l)}_{L,r,0}$ can be estimated according to (2.9) by

$$\bar{\Sigma}^{(l)}_{L,r,0} \subset \{\lfloor r/2^{L-l} \rfloor - 2s, \dots, \lfloor r/2^{L-l} \rfloor + 2s\} \subset \{k-2s, \dots, k+2s\} \tag{7.18}$$

for all $r \in \{2^{L-l}k, \dots, 2^{L-l}(k+1)-1\}$.

The reconstruction stencil is chosen according to Lemma 5.10, i.e.,

$$\mathcal{S}_{l,k} = \{\underline{k}, \dots, \overline{k}\} = \{\underline{k}, \dots, \underline{k}+N\} \tag{7.19}$$

for some $\underline{k} \in \{k-N, \dots, k\}$. Then we obtain by (7.18) and (7.19) the inclusion

$$\bar{\Sigma}^{(l)}_{L,r,0} \setminus \mathcal{S}_{l,k} = \{k-2s, \dots, \underline{k}-1\} \cup \{\overline{k}+1, \dots, k+2s\} =: \Sigma^- \cup \Sigma^+.$$

According to Lemma 5.10 the difference of the averages can be estimated by a linear combination of finite differences of degree $N+1$, i.e.,

$$|v_{l,k'} - \hat{P}_{l,k'}| \lesssim \begin{cases} \max_{k^- = k', \dots, \underline{k}-1} \{|\Delta_1^{N+1} v_{l,k^-}|\} & , \quad k' \in \Sigma^- \\ \max_{k^+ = \overline{k}-N, \dots, k'-N-1} \{|\Delta_1^{N+1} v_{l,k^+}|\} & , \quad k' \in \Sigma^+ \end{cases} \tag{7.20}$$

because the coefficients $\alpha_{k',j}$ only depend on $N$ and the number of summands is uniformly bounded by $\underline{k} - k' \le k - (k-2s) = 2s$ for $k' \in \Sigma^-$ and $k' - \overline{k} \le k + 2s - (k - N + N) = 2s$ for $k' \in \Sigma^+$, respectively.

Since $N \le 2s$ and $k^\pm \in \{k-2s, \dots, k+2s-N-1\}$ for $k^\pm \in \Sigma^\pm$ we may now apply Lemma 5.12, i.e.,

$$\left|\Delta_1^{N+1} v_{l,k^\pm}\right| \lesssim \varepsilon_l^{\min\left(\frac{N+1}{R},1\right)}.$$

Finally, we obtain with (7.20)

$$\left|v_{l,k'} - \hat{P}_{l,k'}\right| \lesssim \varepsilon_l^{\min\left(\frac{N+1}{R},1\right)} \tag{7.21}$$

for $k' \in \tilde{\Sigma}^{(l)}_{L,r,0} \setminus \mathcal{S}_{l,k}$.

Then we conclude from (7.13), (7.16), (7.17) and (7.21)

$$\left|\langle R^N_{l,k'}, \tilde{\varphi}_{l,r}\rangle - v_{L,r}\right| \lesssim \max_{k' \in \bar{\Sigma}^{(l)}_{L,r,0} \setminus \mathcal{S}_{l,k}} \left|\hat{P}_{l,k'} - v_{l,k'}\right| + \varepsilon_l \lesssim \max\left(\varepsilon_l^{\min\left(\frac{N+1}{R},1\right)}, \varepsilon_l\right)$$

provided that the subdivision scheme converges, i.e., Theorem 2.1 holds. ∎

### 7.6. Proof of Lemma 5.15.

*Proof.* We want to estimate the $R$-th derivative of the composite function $G$ by means of finite differences of possibly lower order. For this purpose we first note that by the chain rule for differentiation the derivative can be represented as

$$G^{(R)}(x) = \sum_{m=1}^{R} S^{(m)}(\mathcal{V}(x)) \sum_{\substack{\mathbf{j} \in \{1,\dots,R-m+1\}^m \\ j_1 + \dots + j_m = R}} c_{\mathbf{j},m} \prod_{i=1}^{m} \mathcal{V}^{(j_i)}(x).$$

Here we need the smoothness of the source function $S$ according to Assumption 1. If $\mathcal{V}(x) \in \partial D_i$, then we consider the one-sided continuous extension of the derivatives. Then we can estimate the $R$-th derivative by

$$\sup_{x \in V_{l,k}} |G^{(R)}(x)| \lesssim \sup_{x \in V_{l,k}} \left\{ \prod_{\mu=1}^{R} |\mathcal{V}^{(j_\mu)}(x)|^{k_\mu};\ (\mathbf{j},\mathbf{k}) \in I(R) \right\}, \tag{7.22}$$

up to a constant depending only on the coefficients $c_{\mathbf{j},m}$ and $R$, respectively, and the bounds $\sup_{x \in V_{l,k}} |S^{(m)}(\mathcal{V}(x))|$. The set $I(R)$ is defined in (5.13). From the definition of the sliding average $\mathcal{V}$ and the Lagrangian representation of the interpolation polynomials $Q^{N+1}_{l,k}$ we conclude that there exists a uniform bound such that

$$\sup_{x \in V_{l,k}} |\mathcal{V}(x)| \lesssim \|\check{\mathbf{v}}^n_L\|_{l^\infty}.$$

According to Lemma 5.3 we know that the modified adaptive scheme is uniformly bounded in the sup-norm. Hence the constants only depend on $\tau$ and $\|u\|_{L^\infty}$.

We now consider the Newton representation of the interpolation polynomial $Q_{l,k}^{N+1}$, i.e.,

$$Q_{l,k}^{N+1}(x) = \sum_{\nu=0}^{N+1} W[\underline{k},\dots,\underline{k}+\nu] \prod_{i=0}^{\nu-1}(x - x_{l,\underline{k}+i}).$$

Here $W[\underline{k},\dots,\underline{k}+\nu]$ denotes the $\nu$-th divided difference of the primitive function $W$ to cell $V_{l,k}$. It is converted to the $\nu$-th finite difference of the cell averages by

$$W[\underline{k},\dots,\underline{k}+\nu] = \frac{1}{\nu! h_l^\nu} \sum_{j=0}^{\nu-1} \binom{\nu-1}{j} (-1)^j \left( W(x_{l,\underline{k}+\nu-j}) - W(x_{l,\underline{k}+\nu-j-1}) \right) =$$

$$\frac{1}{\nu! h_l^{\nu-1}} \sum_{j=0}^{\nu-1} \binom{\nu-1}{j} (-1)^j v_{l,\underline{k}+\nu-j-1} = \frac{1}{\nu! h_l^{\nu-1}} (-1)^{\nu-1} \Delta_1^{\nu-1} v_{l,\underline{k}}. \tag{7.23}$$

Since the $j$-th derivative of the interpolation polynomial is determined by

$$\left(\frac{d}{dx}\right)^{(j)} Q_{l,k}^{N+1}(x) = \sum_{\nu=j}^{N+1} W[\underline{k},\dots,\underline{k}+\nu] \left(\frac{d}{dx}\right)^{(j)} \left( \prod_{i=0}^{\nu-1}(x - x_{l,\underline{k}+i}) \right)$$

the $j$-th derivative of the sliding average is

$$\mathcal{V}^{(j)}(x) = \frac{1}{h_L} \sum_{\nu=j+1}^{N+1} W[\underline{k},\dots,\underline{k}+\nu] \int_{x-h_L/2}^{x+h_L/2} \left(\frac{d}{dz}\right)^{(j+1)} \left( \prod_{i=0}^{\nu-1}(z - x_{l,\underline{k}+i}) \right) dz.$$

The integral of the right-hand side can be estimated by

$$\sup_{x\in V_{l,k}} \left| \int_{x-h_L/2}^{x+h_L/2} \left(\frac{d}{dz}\right)^{(j-1)} \left( \prod_{i=0}^{\nu-1}(z - x_{l,\underline{k}+i}) \right) dz \right| \lesssim h_L h_l^{\nu-j+1}.$$

Together with (7.23) we obtain

$$\sup_{x\in V_{l,k}} |\mathcal{V}^{(j)}(x)| \lesssim \sum_{\nu=j+1}^{N+1} \frac{1}{\nu!} \frac{1}{h_l^{\nu-1}} |\Delta_1^{\nu-1} v_{l,\underline{k}}| h_l^{\nu-j+1} \lesssim h_l^{2-j} \max_{\nu=j+1,\dots,N+1} |\Delta_1^{\nu-1} v_{l,\underline{k}}|. \tag{7.24}$$

By means of induction and using the addition theorem for binomial coefficients we notice that

$$\Delta_1^{\nu+j} v_{l,\underline{k}} = \sum_{i=0}^{\nu} \binom{\nu}{i} (-1)^i \Delta_1^j v_{l,\underline{k}+i}, \quad \nu \geq 0.$$

Then we deduce from (7.24)

$$\sup_{x\in V_{l,k}} |\mathcal{V}^{(j)}(x)| \lesssim h_l^{2-j} \max_{i=0,\dots,N-j} |\Delta_1^j v_{l,\underline{k}+i}|, \quad j \leq R. \tag{7.25}$$

Combining (7.22) and (7.25) we obtain

$$\sup_{x\in V_{l,k}} |G^{(R)}(x)| \lesssim \sup_{x\in V_{l,k}} \left\{ \prod_{\mu=1}^{R} \left( h_l^{2-j_\mu} |\Delta_1^{j_\mu} v_{l,\underline{k}+\nu_\mu}| \right)^{k_\mu} ;\ (\mathbf{j},\underline{k}) \in I(R),\ \nu \in I(R,\mathbf{j}) \right\}, \tag{7.26}$$

where $I(R,\mathbf{j}) := \{\nu;\, \nu_\mu \in \{0,\dots,N-j_\mu\}^R$.

It now remains to estimate the finite differences on the right-hand side of (7.26) by means of Lemma 5.12. For this purpose we verify that $\underline{k}+\nu \in \{k-2s,\dots,k+2s-j\}$ for $\nu \in \{0,\dots,N-j\}$. Obviously, this holds true if $1 \le N \le 2s$ and $\underline{k} \in \{k-N,\dots,k\}$. Then we infer from Lemma 5.12

$$|\Delta_1^j v_{l,\underline{k}+\nu}| \lesssim \varepsilon_l^{\min(j/R,1)}.$$

We now employ this in (7.26) and obtain

$$\prod_{\mu=1}^R |\Delta_1^{j_\mu} v_{\underline{k}+\nu_\mu}|^{k_\mu} \lesssim \varepsilon_l^{\sum_{\mu=1}^R j_\mu k_\mu/R} = \varepsilon_l. \tag{7.27}$$

On the other hand, we have

$$\prod_{\mu=1}^R h_l^{(2-j_\mu)k_\mu} = h_l^{2\sum_{\mu=1}^R k_\mu - \sum_{\mu=1}^R j_\mu k_\mu} \le h_l^{2-R}, \tag{7.28}$$

because $\sum_{\mu=1}^R j_\mu k_\mu = R$ and $\sum_{\mu=1}^R k_\mu \ge 1$. Inserting (7.27) and (7.28) in (7.26) yields the assertion. ∎